The Star Formation Newsletter

A community newsletter on Star and Planet Formation research

No. 354 — 30 June 2022
Editor: João Alves
www.starformation.news

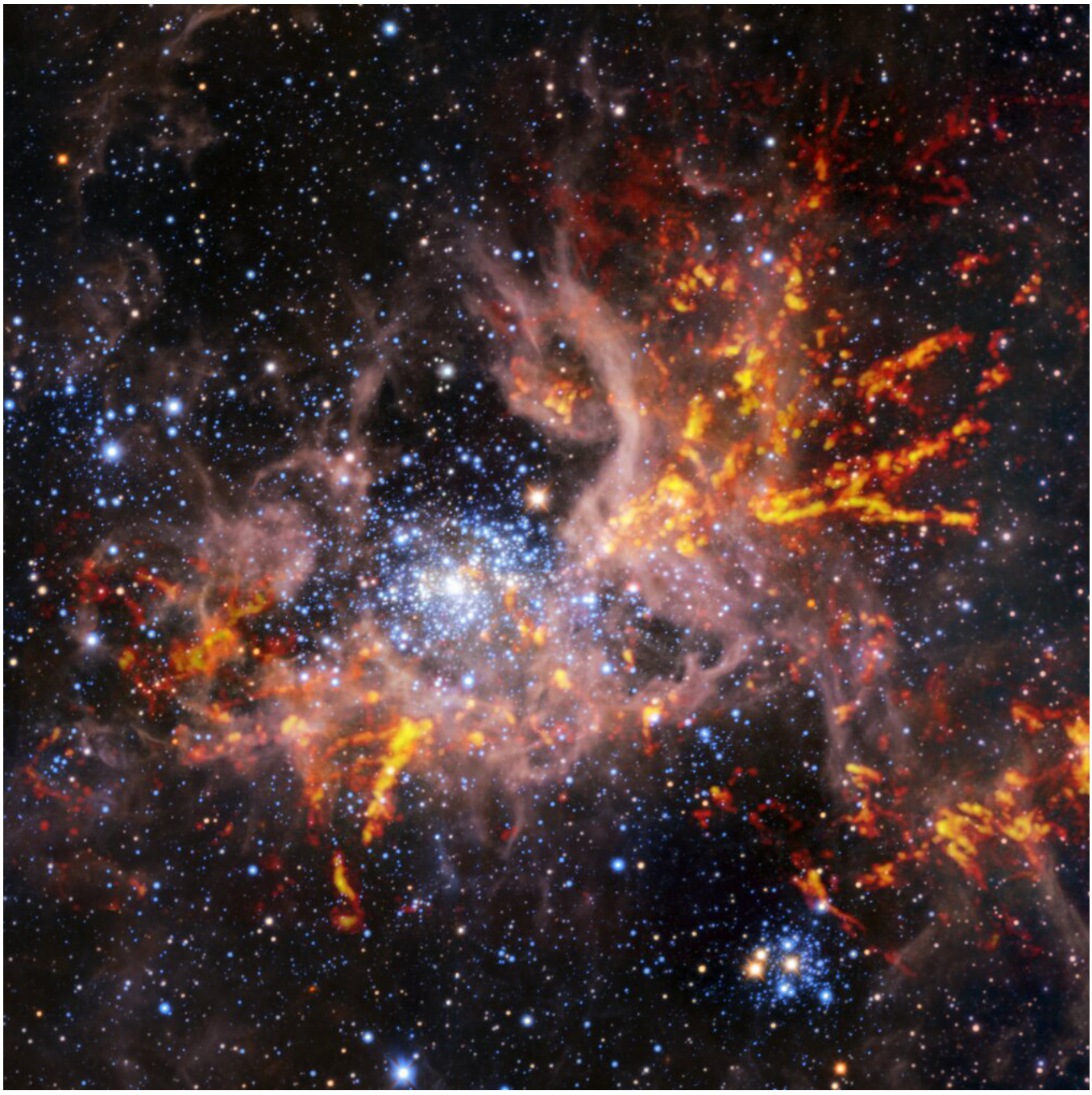

Links to sections

Cover image caption

30 Dor in the Large Magellanic Cloud (or the Tarantula Nebula) is the most active starburst region in the Local Group of galaxies. With an apparent magnitude of 8, 30 Dor is an extremely luminous non-stellar object. The Tarantula Nebula would cast visible shadows if it were as close to Earth as the Orion Nebula. This composite image background is a series of NIR images. The bright red-yellow streaks superimposed on the background NIR image come from CO observations taken by ALMA, revealing complex filamentary networks stretching away approximately, from the central cluster, not unlike an upscaled version of the Orion Nebula Cluster. Credit: ESO, ALMA (ESO/NAOJ/NRAO)/Wong et al. 2022, ESO/M.-R. Cioni/VISTA Magellanic Cloud survey.

Note from the Editor

The Star Formation Newsletter is now on the web at **www.starformation.news**. This PDF file contains the monthly Abstracts and links to the different Newsletter sections. Red text in this PDF is a url link. Submitting an abstract to the SFN is as simple as entering the arXiv ID (e.g., 2006.10139) in a web form on the SFN web site. **Do not remove the LaTeX formatting when submitting to the arXiv**. If you do, your abstract will not look great either at the arXiv or the SFN.

Abstracts

1. The origin of the [CII]-deficit in a simulated dwarf galaxies starburst

Thomas G. Bisbas, Stefanie Walch, Thorsten Naab, Natalia Lahén, Rodrigo Herrera-Camus, Ulrich P. Steinwandel, Constantina M. Fotopoulou, Chia-Yu Hu, Peter H. Johansson ★
We present [CII] synthetic observations of smoothed particle hydrodynamics (SPH) simulations of a dwarf galaxy merger. The merging process varies the star-formation rate by more than three orders of magnitude. Several star clusters are formed, the feedback of which disperses and unbinds the dense gas through expanding HII regions and supernova (SN) explosions. For galaxies with properties similar to the modelled ones, we find that the [CII] emission remains optically thin throughout the merging process. We identify the Warm Neutral Medium ($3 < \log T_{\rm gas} < 4$ with $\chi_{\rm HI} > 2\chi_{\rm H2}$) to be the primary source of [CII] emission ($\sim 58\%$ contribution), although at stages when the HII regions are young and dense (during star cluster formation or SNe in the form of ionized bubbles) they can contribute $\gtrsim 50\%$ to the total [CII] emission. We find that the [CII]/FIR ratio decreases due to thermal saturation of the [CII] emission caused by strong FUV radiation fields emitted by the massive star clusters, leading to a [CII]-deficit medium. We investigate the [CII]-SFR relation and find an approximately linear correlation which agrees well with observations, particularly those from the Dwarf Galaxy Survey. Our simulation reproduces the observed trends of [CII]/FIR versus $\Sigma_{\rm SFR}$ and $\Sigma_{\rm FIR}$, and it agrees well with the Kennicutt relation of SFR-FIR luminosity. We propose that local peaks of [CII] in resolved observations may provide evidence for ongoing massive cluster formation.

2. Infrared Spectroscopy of free-floating planet candidates in Upper Scorpius and Ophiuchus

H. Bouy, M. Tamura, D. Barrado, K. Motohara, N. Castro Rodríguez, N. Miret-Roig, M. Konishi, S. Koyama, H. Takahashi, N. Huelamo, E. Bertin, J. Olivares, L. M. Sarro, A. Berihuete, J. -C. Cuillandre, P. A. B. Galli, Y. Yoshii, T. Miyata ★
Context: A rich population of low-mass brown dwarfs and isolated planetary mass objects has been reported recently in the Upper Scorpius and Ophiuchus star forming complex. Aims: We investigate the membership, nature and properties of 17 of these isolated planetary mass candidates using low-resolution near-infrared spectra. Methods: We investigate the membership by looking for evidences of youth using four diagnostics: the slope of the continuum between the J and Ks band, the Hcont and TLI-g gravity sensitive indices, and by comparing the spectra to young and field (old) M and L-dwarf standards. Results: All the targets but one are confirmed as young ultracool objects, with spectral types between L0 and L6 and masses in the range 0.004-0.013 M according to evolutionary models. The status of the last target is unclear at this point. Conclusions: Only one possible contaminant has been identified among the 17 targets, suggesting that the contamination level of the original sample must be lower than 6%

3. Collisional Charging in the Low Pressure Range of Protoplanetary Disks

T. Becker, T. Steinpilz, J. Teiser, G. Wurm ★ In recent years, collisional charging has been proposed to promote the growth of pebbles in early phases of planet formation. Ambient pressure in protoplanetary disks spans a wide range from below 10^{-9} mbar up to way beyond mbar. Yet, experiments on collisional charging of same material surfaces have only been conducted under Earth atmospheric pressure, Martian pressure and more generally down to 10^{-2} mbar thus far. This work presents first pressure dependent charge measurements of same material collisions between 10^{-8} and 10^{3} mbar. Strong charging occurs down to the lowest pressure. In detail, our observations show a strong similarity to the pressure dependence of the breakdown voltage between two electrodes and we suggest that breakdown also determines the maximum charge on colliding grains in protoplanetary disks. We conclude that collisional charging can occur in all parts of protoplanetary disks relevant for planet formation.

4. HCN snowlines in protoplanetary disks: constraints from ice desorption experiments

Jennifer B. Bergner, Mahesh Rajappan, Karin I. Oberg ★ HCN is among the most commonly detected molecules in star- and planet-forming regions. It is of broad interest as a tracer of star-formation physics, a probe of nitrogen astrochemistry, and an ingredient in prebiotic chemical schemes. Despite this, one of the most fundamental astrochemical properties of HCN remains poorly characterized: its thermal desorption behavior. Here, we present a series of experiments to characterize the thermal desorption of HCN in astrophysically relevant conditions, with a focus on predicting the HCN sublimation fronts in protoplanetary disks. We derive HCN-HCN and HCN-H2O binding energies of 3207±197 K and 4192±68 K, which translate to disk midplane sublimation temperatures around 85 K and 103 K. For a typical midplane temperature profile, HCN should only begin to sublimate 1-2 au exterior to the H2O snow line. Additionally, in H2O-dominated mixtures (20:1 H2O:HCN), we find that the majority of HCN remains trapped in the ice until H2O crystallizes. Thus, HCN may be retained in disk ices at almost all radii where H2O-rich planetesimals form. This implies that icy body impacts to planetary surfaces should commonly deliver this potential prebiotic ingredient. A remaining unknown is the extent to which HCN is pure or mixed with H2O in astrophysical ices, which impacts the HCN desorption behavior as well as the outcomes of ice-phase chemistry. Pure HCN and HCN:H2O mixtures exhibit distinct IR bands, raising the possibility that the James Webb Space Telescope will elucidate the mixing environment of HCN in star- and planet-forming regions and address these open questions.

5. Transit Hunt for Young and Maturing Exoplanets (THYME) VIII: a Pleiades-age association harboring two transiting planetary systems from Kepler

Madyson G. Barber, Andrew W. Mann, Jonathan L. Bush, Benjamin M. Tofflemire, Adam L. Kraus, Daniel M. Krolikowski, Andrew Vanderburg, Matthew J. Fields, Elisabeth R. Newton, Dylan A. Owens, Pa Chia Thao ★ Young planets provide a window into the early stages and evolution of planetary systems. Ideal planets for such research are in coeval associations, where the parent population can precisely determine their ages. We describe a young association (MELANGE-3) in the Kepler field, which harbors two transiting planetary systems (Kepler-1928 and Kepler-970). We identify MELANGE-3 by searching for kinematic and spatial overdensities around Kepler planet hosts with high levels of lithium. To determine the age and membership of MELANGE-3, we combine new high-resolution spectra with archival light curves, velocities, and astrometry of stars near Kepler-1928 spatially and kinematically. We use the resulting rotation sequence, lithium levels, and color-magnitude diagram of candidate members to confirm the presence of a coeval 105±10 Myr population. MELANGE-3 may be part of the recently identified Theia 316 stream. For the two exoplanet systems, we revise the stellar and planetary parameters, taking into account the newly-determined age. Fitting the 4.5 yr Kepler light curves, we find that Kepler-1928 b is a $2.0 \pm 0.1 R_{\oplus}$ planet on a 19.58-day orbit, while Kepler-970 b is a $2.8 \pm 0.2 R_{\oplus}$ planet on a 16.73-day orbit. Kepler-1928 was previously flagged as an eclipsing binary, which we rule out using radial velocities from APOGEE and statistically validate the signal as planetary in origin. Given its overlap with the Kepler field, MELANGE-3 is valuable for studies of spot evolution on year timescales, and both planets contribute to the growing work on transiting planets in young stellar associations.

6. A new phase of massive star formation? A luminous outflow cavity centred on an infrared quiet core

L. Bonne, N. Peretto, A. Duarte-Cabral, A. Schmiedeke, N. Schneider, S. Bontemps, A. Whitworth ★ We present APEX, infrared and radio continuum observations of the G345.88-1.10 hub filament system which is a newly discovered star-forming cloud that hosts an unusually bright bipolar infrared nebulosity at its centre. At a distance of $2.26^{+0.30}_{-0.21}$ kpc, G345.88-1.10 exhibits a network of parsec-long converging filaments. At the junction of these filaments lie four infrared-quiet fragments. The densest fragment (with M=210 $M_{\odot}$, $R_{\rm eff}$ = 0.14 pc) sits at the centre of a wide (opening angle of $\sim 90 \pm 15^{o}$) bipolar nebulosity. ^{12}CO(2-1) observations show that these infrared-bright nebulosities are spatially associated with a powerful molecular outflow from the central fragment. Negligible radio continuum and no H30α emission is detected towards the cavities, seemingly excluding that ionising radiation drives the evolution of the cavities. Furthermore, radiative transfer simulations are unable to reproduce the observed combination of a low-luminosity ($\lesssim$ 500 $L_{\odot}$) central source and a surrounding high-luminosity ($\sim$ 4000 $L_{\odot}$) mid-infrared-bright bipolar cavity. This suggests that radiative heating from a central protostar cannot

be responsible for the illumination of the outflow cavities. To our knowledge, this is the first reported object of this type. The rarity of objects like G345.88-1.10 is likely related to a very short phase in the massive star and/or cluster formation process that was so far unidentified. We discuss whether mechanical energy deposition by one episode or successive episodes of powerful mass accretion in a collapsing hub might explain the observations. While promising in some aspects, a fully coherent scenario that explains the presence of a luminous bipolar cavity centred on an infrared-dark fragment remains elusive at this point.

7. Resolving desorption of complex organic molecules in a hot core: Transition from non-thermal to thermal desorption or two-step thermal desorption?

Laura A. Busch, Arnaud Belloche, Robin T. Garrod, Holger S. P. Müller, Karl M. Menten ★ Using the high angular resolution provided by the ALMA interferometre we want to resolve the COM emission in the hot molecular core Sagittarius B2(N1) and thereby shed light on the desorption process of Complex Organic Molecules (COMs) in hot cores. We use data taken as part of the 3 mm spectral line survey Re-exploring Molecular Complexity with ALMA (ReMoCA) to investigate the morphology of COM emission in Sagittarius B2(N1). Spectra of ten COMs are modelled under the assumption of LTE and population diagrams are derived for positions at various distances to the south and west from the continuum peak. Based on this analysis, resolved COM rotation temperature and COM abundance profiles are derived. Based on the morphology, a rough separation into O- and N-bearing COMs can be done. Temperature profiles are in agreement with expectations of protostellar heating of an envelope with optically thick dust. Abundance profiles reflect a similar trend as seen in the morphology and, to a great extent, agree with results of astrochemical models that, besides the co-desorption with water, predict that O-bearing COMs are mainly formed on dust grain surfaces at low temperatures while at least some N-bearing COMs and CH_3CHO are substantially formed in the gas phase at higher temperatures. Our observational results, in comparison with model predictions, suggest that COMs that are exclusively or to a great extent formed on dust grains desorb thermally at 100 K from the grain surface likely alongside water. Non-zero abundance values below 100 K suggest that another desorption process is at work at these low temperatures: either non-thermal desorption or partial thermal desorption related to lower binding energies experienced by COMs in the outer, water-poor ice layers. In either case, this is the first time that the transition between two regimes of COM desorption has been resolved in a hot core.

8. Orbital parameters and activity of ZZ Tau – a low mass young binary with circumbinary disc

A. Belinski, M. Burlak, A. Dodin, N. Emelyanov, N. Ikonnikova, S. Lamzin, B. Safonov, A. Tatarnikov ★ We present the results of our new observations of the young binary ZZ Tau with a circumbinary disc. The system was found to consist of two coeval (age < 2 Myr) classical T Tauri stars with the total mass 0.86 ± 0.09 $M_\odot$, orbital period 46.8 ± 0.8 yr, semimajor axis 88.2 ± 2.1 mas, eccentricity 0.58 ± 0.02 and the orbital inclination $123.^\circ8 \pm 1.^\circ0$. The accretion rate of ZZ Tau A and ZZ Tau B are approximately 7×10^{-10} and 2×10^{-10} $M_\odot$ yr^{-1}, respectively. No correlation was found between the long-term photometric variability of ZZ Tau and orbital position of its components. The periodic light variations with $P = 4.171 \pm 0.002$ days was observed in the $BVRI$ bands presumably connected with an accretion (hot) spot on the surface of the primary (ZZ Tau A). At the same time no periodicity was observed in the U band nor in the emission line profile variations probably due to the significant contribution of ZZ Tau B's emission, which dominates shortward of $\lambda \approx 0.4\,\mu$m. We argue that the extinction in the direction to the primary is noticeably larger than that to the secondary. It appeared that the rotation axis of the primary is inclined to the line of sight by $\approx 31^\circ \pm 4^\circ$. We concluded also that ZZ Tau is the source of an CO molecular outflow, however, ZZ Tau IRS rather than ZZ Tau is the source of the Herbig-Haro object HH393.

9. The signature of large scale turbulence driving on the structure of the interstellar medium

Tine Colman, Jean-François Robitaille, Patrick Hennebelle, Marc-Antoine Miville-Deschênes, Noé Brucy, Ralf S. Klessen, Simon C. O. Glover, Juan D. Soler, Davide Elia, Alessio Traficante, Sergio Molinari, Leonardo Testi ★ The mechanisms that maintain turbulence in the interstellar medium (ISM) are still not identified. This work investigates how we can distinguish between two fundamental driving mechanisms: the accumulated effect of stellar feedback versus the energy injection from Galactic scales. We perform a series of numerical simulations describing a stratified star forming ISM subject to self-consistent stellar feedback. Large scale external turbulent driving of various intensities is added to mimic galactic driving mechanisms. We analyse the resulting column density maps with a technique called Multi-scale non-Gaussian segmentation that separates the coherent structures and the Gaussian background. This effectively discriminates between the various simulations and is a promising method to understand the ISM structure. In particular the power spectrum of the coherent structures flattens above 60 pc when turbulence is driven only by stellar feedback. When large-scale driving is applied, the turn-over shifts to larger scales. A systematic comparison with the Large Magellanic Cloud (LMC) is then performed. Only 1 out of 25 regions has a coherent power spectrum which is consistent with the feedback-only simulation. A detailed study of the turn-over scale leads us to conclude that regular stellar feedback is not enough to explain the observed ISM structure on scales larger than 60 pc. Extreme feedback in the form of supergiant shells likely plays an important role but cannot explain all the

regions of the LMC. If we assume ISM structure is generated by turbulence, another large scale driving mechanism is needed to explain the entirety of the observations.

10. The Twisted Magnetic Field of the Protobinary L483

Erin G. Cox, Giles Novak, Sarah Sadavoy, Leslie W. Looney, Dennis Lee, Marc Berthoud, Tyler L. Bourke, Simon Coudé, Frankie Encalada, Laura M. Fissel, Rachel Harrison, Martin Houde, Zhi-Yun Li, Philip C. Myers, Kate Pattle, Fabio P. Santos, Ian W. Stephens, Hailin Wang, Sebastian Wolf ★ We present H-band (1.65 μm) and SOFIA HAWC+ 154 μm polarization observations of the low-mass core L483. Our H-band observations reveal a magnetic field that is overwhelmingly in the E-W direction, which is approximately parallel to the bipolar outflow that is observed in scattered IR light and in single-dish ^{12}CO observations. From our 154 μm data, we infer a $\sim 45^{\circ}$ twist in the magnetic field within the inner 5" (1000 au) of L483. We compare these new observations with published single-dish 350 μm polarimetry and find that the 10,000 au scale H-band data match the smaller scale 350 μm data, indicating that the collapse of L483 is magnetically regulated on these larger scales. We also present high-resolution 1.3 mm ALMA data of L483 which reveals it is a close binary star with a separation of 34 au. The plane of the binary of L483 is observed to be approximately parallel to the twisted field in the inner 1000 au. Comparing this result to the $\sim$ 1000 au protostellar envelope, we find that the envelope is roughly perpendicular to the 1000 au HAWC+ field. Using the data presented, we speculate that L483 initially formed as a wide binary and the companion star migrated to its current position, causing an extreme shift in angular momentum thereby producing the twisted magnetic field morphology observed. More observations are needed to further test this scenario.

11. Discovery of the cyclic C5H radical in TMC-1

Carlos Cabezas, Marcelino Agundez, Raul Fuentetaja, Yasuki Endo, Nuria Marcelino, Belen Tercero, Juan R. Pardo, Pablo de Vicente, Jos Cernicharo ★ Cyclic C5H (c-C5H), the radical formed by substituting an ethynyl group CCH for the hydrogen atom in the c-C3H radical, has been detected for the first time in the space. The c-C5H species is an isomer of the well-known linear radical l-C5H and is 6 kcal/mol less stable. A total of 17 rotational transitions were detected for the c-C5H species in TMC-1 within the 31.0-50.3 GHz range using the Yebes 40m radio telescope. We derive a column density of (9.0 +/- 0.9)e10 cm-2 for c-C5H. Additionally, we observed 12 lines for l-C5H and derive a column density for it of (1.3 +/- 0.3)e12 cm-2, which results in an abundance ratio c-C5H/l-C5H of 0.069. This is in sharp contrast with the value found for the analogue system c-C3H/l-C3H, whose ratio is 5.5 in TMC-1. We discuss the formation of c-C5H and conclude that this radical is probably formed in the reaction of atomic carbon with diacetylene.

12. The Doppler-flip in HD100546 as a disk eruption: the elephant in the room of kinematic protoplanet searches

Simon Casassus, Miguel Carcamo, Antonio Hales, Philipp Weber, Bill Dent ★ The interpretation of molecular-line data in terms of hydro dynamical simulations of planet-disk interactions fosters new hopes for the indirect detection of protoplanets. In a model-independent approach, embedded protoplanets should be found at the roots of abrupt Doppler flips in velocity centroid maps. However, the largest velocity perturbation known for an unwarped disk, in the disk of HD100546, leads to a conspicuous Doppler flip that coincides with a thick dust ring, in contradiction with an interpretation in terms of a $>$ 1Mjup body. Here we present new ALMA observations of the 12CO(2-1) kinematics in HD 100546, with a factor of two finer angular resolutions. We find that the disk rotation curve is consistent with a central mass $2.1 < M^* /Msun < 2.3$, and that the blue-shifted side of the Doppler flip is due to vertical motions, reminiscent of the disk wind proposed previously from blue-shifted SO lines. We tentatively propose a qualitative interpretation in terms of a surface disturbance to the Keplerian flow, i.e. a disk eruption, driven by an embedded outflow launched by a 10Mearth body. Another interpretation involves a disk-mass-loading hot-spot at the convergence of an envelope accretion streamer.

13. Organic chemistry in the first phases of Solar-type protostars

C. Ceccarelli, C. Codella, N. Balucani, D. Bockelée-Morvan, E. Herbst, C. Vastel, P. Caselli, C. Favre, B. Lefloch, K. Öberg ★ Planetary systems such as our own are formed after a long process where matter condenses from diffuse clouds to stars, planets, asteroids, comets and residual dust, undergoing dramatic changes in physical and chemical state in less than a few million years. Several studies have shown that the chemical composition during the early formation of a Solar-type planetary system is a powerful diagnostic to track the history of the system itself. Among the approximately 270 molecules so far detected in the ISM, the so-called interstellar complex organic molecules (iCOMs) are of particular interest both because of their evolutionary diagnostic power and because they might be potential precursors of biomolecules, which are at the basis of terrestrial life. This Chapter focuses on the evolution of organic molecules during the early stages of a Solar-type planetary system, represented by the prestellar, Class 0/I and protoplanetary disk phases, and compares them with what is observed presently in Solar System comets. Our twofold goal is to review the processes at the base of organic chemistry during Solar-type star formation and, in addition, to possibly provide constraints on the early history of our own planetary system.

14. FAUST VI. VLA 1623–2417 B: a new laboratory for astrochemistry around protostars on 50 au scale

C. Codella, A. López-Sepulcre, S. Ohashi, C. J. Chandler, M. De Simone, L. Podio, C. Ceccarelli, N. Sakai, F. Alves, A. Durán, D. Fedele, L. Loinard, S. Mercimek, N. Murillo, E. Bianchi, M. Bouvier, G. Busquet, P. Caselli, F. Dulieu, S. Feng, T. Hanawa, D. Johnstone, B. Lefloch, L. T. Maud, G. Moellenbrock, Y. Oya, B. Svoboda, S. Yamamoto ★ The ALMA interferometer, with its unprecedented combination of high-sensitivity and high-angular resolution, allows for (sub-)mm wavelength mapping of protostellar systems at Solar System scales. Astrochemistry has benefited from imaging interstellar complex organic molecules in these jet-disk systems. Here we report the first detection of methanol (CH3OH) and methyl formate (HCOOCH3) emission towards the triple protostellar system VLA1623-2417 A1+A2+B, obtained in the context of the ALMA Large Program FAUST. Compact methanol emission is detected in lines from Eu = 45 K up to 61 K and 537 K towards components A1 and B, respectively. LVG analysis of the CH3OH lines towards VLA1623-2417 B indicates a size of 0.11-0.34 arcsec (14-45 au), a column density N(CH3OH) = $10^{16} - 10^{17}$ cm^{-2}, kinetic temperature > 170 K, and volume density > 10^8 cm^{-3}. An LTE approach is used for VLA1623-2417 A1, given the limited Eu range, and yields Trot < 135 K. The methanol emission around both VLA1623-2417 A1 and B shows velocity gradients along the main axis of each disk. Although the axial geometry of the two disks is similar, the observed velocity gradients are reversed. The CH3OH spectra from B shows two broad (4-5 km/s) peaks, which are red- and blue-shifted by about 6-7 km/s from the systemic velocity. Assuming a chemically enriched ring within the accretion disk, close to the centrifugal barrier, its radius is calculated to be 33 au. The methanol spectra towards A1 are somewhat narrower (about 4 km/s), implying a radius of 12-24 au.

15. Stellar collisions in globular clusters: Constraints on the initial mass function of the first generation of stars

Sami Dib, Valery V. Kravtsov, Hosein Haghi, Akram Hasani Zonoozi, José Antonio Belinchón ★ Globular clusters display an anticorrelation between the fraction of the first generation of stars (N(G1)/N(tot)) and the slope of the present-day mass function of the clusters (α_{pd}), which is particularly significant for massive clusters. In the framework of the binary-mediated collision scenario for the formation of the second-generation stars in globular clusters, we test the effect of a varying stellar initial mass function (IMF) of the G1 stars on the (N(G1)/N(tot)) − α_{pd} anticorrelation. We use a simple collision model that has only two input parameters, the shape of the IMF of G1 stars and the fraction of G1 stars that coalesce to form second-generation stars. We show that a variable efficiency of the collision process is necessary in order to explain the (N(G1)/N(tot)) − α_{pd} anticorrelation; however, the scatter in the anticorrelation can only be explained by variations in the IMF, and in particular by variations in the slope in the mass interval ≈ (0.1-0.5) M$_\odot$. Our results indicate that in order to explain the scatter in the (N(G1)/N(tot)) − α_{pd} relation, it is necessary to invoke variations in the slope in this mass range between ≈ −0.9 and ≈ −1.9. Interpreted in terms of a Kroupa-like broken power law, this translates into variations in the mean mass of between ≈ 0.2 and 0.55 M$_\odot$. This level of variation is consistent with what is observed for young stellar clusters in the Milky Way and may reflect variations in the physical conditions of the globular cluster progenitor clouds at the time the G1 population formed or may indicate the occurrence of collisions between protostellar embryos before stars settle on the main sequence.

16. Clumpy accretion in pre-main-sequence stars as a source of perturbations in circumstellar disks

Tatiana V. Demidova, Vladimir P. Grinin ★ The development of perturbations in the circumstellar disks of pre-main-sequence stars caused by clumpy accretion was investigated. Here we perform 3D hydrodynamical smoothed particle hydrodynamics simulations of disks perturbed by a recent clump accretion event. These simulations are further explored by radiative transfer calculations to quantify the observational appearance of such disks. It was shown that the density waves in the disks were formed at the fall of the clump. After several revolutions they can transform into spirals and ring structures. Their images in millimeter wavelengths are very similar to those observed with Atacama Large Millimeter/submillimeter Array in some protoplanetary disks. We assume that clumpy accretion may be the source of such structures.

17. In-depth direct imaging and spectroscopic characterization of the young Solar System analog HD 95086

C. Desgrange et al. ★ Context. HD 95086 is a young nearby Solar System analog hosting a giant exoplanet orbiting at 57 au from the star between an inner and outer debris belt. The existence of additional planets has been suggested as the mechanism that maintains the broad cavity between the two belts. Aims. We present a dedicated monitoring of HD 95086 with the VLT/SPHERE instrument to refine the orbital and atmospheric properties of HD 95086 b, and to search for additional planets in this system. Methods. SPHERE observations, spread over ten epochs from 2015 to 2019 and including five new datasets, were used. Combined with archival observations, from VLT/NaCo (2012-2013) and Gemini/GPI (2013-2016), the extended set of astrometric measurements allowed us to refine the orbital properties of HD 95086 b. We also investigated the spectral properties and the presence of a circumplanetary disk around HD 95086 b by using the special fitting tool exploring

the diversity of several atmospheric models. In addition, we improved our detection limits in order to search for a putative planet c via the K-Stacker algorithm. Results. We extracted for the first time the JH low-resolution spectrum of HD 95086 b by stacking the six best epochs, and confirm its very red spectral energy distribution. Combined with additional datasets from GPI and NaCo, our analysis indicates that this very red color can be explained by the presence of a circumplanetary disk around planet b, with a range of high-temperature solutions (1400-1600 K) and significant extinction (Av $>$ 10 mag), or by a super-solar metallicity atmosphere with lower temperatures (800-1300 K), and small to medium amount of extinction (Av $<$ 10 mag). We do not find any robust candidates for planet c, but give updated constraints on its potential mass and location.

18. A Multiwavelength Study of the Sgr B Region: Contiguous Cloud-Cloud Collisions Triggering Widespread Star Formation Events?

Rei Enokiya, Yasuo Fukui ★ The Sgr B region, including Sgr B1 and Sgr B2, is one of the most active star-forming regions in the Galaxy. Hasegawa et al. (1994) originally proposed that Sgr B2 was formed by a cloud-cloud collision (CCC) between two clouds with velocities of $\sim$45 km s^{-1} and $\sim$75 km s^{-1}. However, some recent observational studies conflict with this scenario. We have re-analyzed this region, by using recent, fully sampled, dense-gas data and by employing a recently developed CCC identification methodology, with which we have successfully identified more than 50 CCCs and compared them at various wavelengths. We found two velocity components that are widely spread across this region and that show clear signatures of a CCC, each with a mass of $\sim 10^6$ $M_\odot$. Based on these observational results, we suggest an alternative scenario, in which contiguous collisions between two velocity features with a relative velocity of $\sim$20 km s^{-1} created both Sgr B1 and Sgr B2. The physical parameters, such as the column density and the relative velocity of the colliding clouds, satisfy a relation that has been found to apply to the most massive Galactic CCCs, meaning that the triggering of high-mass star formation in the Galaxy and starbursts in external galaxies can be understood as being due to the same physical CCC process.

19. Gap opening by planets in discs with magnetised winds

Vardan Elbakyan, Yinhao Wu, Sergei Nayakshin, Giovanni Rosotti ★ Planets open deep gaps in protoplanetary discs when their mass exceeds a gap opening mass, $M_{\rm gap}$. We use one- and two-dimensional simulations to study planet gap opening in discs with angular momentum transport powered by MHD disc winds. We parameterise the efficiency of the MHD disc wind angular momentum transport through a dimensionless parameter $\alpha_{\rm dw}$, which is an analogue to the turbulent viscosity $\alpha_{\rm v}$. We find that magnetised winds are much less efficient in counteracting planet tidal torques than turbulence is. For discs with astrophysically realistic values of $\alpha_{\rm dw}$, $M_{\rm gap}$ is always determined by the residual disc turbulence, and is a factor of a few to ten smaller than usually obtained for viscous discs. We introduce a gap opening criterion applicable for any values of $\alpha_{\rm v}$ and $\alpha_{\rm dw}$ that may be useful for planet formation population synthesis. We show that in discs powered by magnetised winds, growing planets detach from the disc at planet masses below $\sim 0.1 M_{\rm Jup}$ inside 10 AU. This promotes formation of super-Earth planets rather than gas giants in this region, in particular precluding formation of hot jupiters in situ. On larger scales, ALMA gap opening planet candidates may be less massive than currently believed. Future high-resolution observations with instruments such as the extended ALMA, ngVLA, and SKA are likely to show abundant narrow annular features at $R < 10$ AU due to ubiquitous super-Earth planets.

20. SIRIUS Project. IV. The formation history of the Orion Nebula Cluster driven by clump mergers

Michiko S. Fujii, Long Wang, Yutaka Hirai, Yoshito Shimajiri, Jun Kumamoto, Takayuki Saitoh ★ The Orion Nebula Cluster (ONC) is an excellent example for understanding the formation of star clusters. Recent studies have shown that ONC has three distinct age populations and anisotropy in velocity dispersions, which are key characteristics for understanding the formation history of the ONC. In this study, we perform a smoothed-particle hydrodynamics/N-body simulation of star cluster formation from a turbulent molecular cloud. In this simulation, stellar orbits are integrated using a high-order integrator without gravitational softening; therefore, we can follow the collisional evolution of star clusters. We find that hierarchical formation causes episodic star formation that is observed in the ONC. In our simulation, star clusters evolve due to mergers of subclumps. The mergers bring cold gas with the clumps into the forming cluster. This enhances the star formation in the cluster centre. The dense cold gas in the cluster centre continues to form stars until the latest time. This explains the compact distribution of the youngest stars observed in the ONC. Subclump mergers also contribute to the anisotropy in the velocity dispersions and the formation of runaway stars. However, the anisotropy disappears within 0.5 Myr. The virial ratio of the cluster also increases after a merger due to the runaways. These results suggest that the ONC recently experienced a clump merger. We predict that most runaways originated from the ONC have already been found, but walkaways have not.

21. The Mysterious Affair of the H_2 in AU Mic

Laura Flagg, Christopher Johns-Krull, Kevin France, Gregory Herczeg, Joan Najita, Allison Youngblood, Adolfo Carvalho, John Carptenter, Scott J. Kenyon, Elisabeth R. Newton, Keighley Rockcliffe ★ Molecular hydrogen is the most abundant molecule in the Galaxy and plays important roles for planets, their circumstellar environments, and many of their host stars. We have confirmed the presence of molecular hydrogen in the AU Mic system using high-resolution FUV spectra from HST-STIS during both quiescence and a flare. AU Mic is a ∼23 Myr M dwarf which hosts a debris disk and at least two planets. We estimate the temperature of the gas at 1000 to 2000 K, consistent with previous detections. Based on the radial velocities and widths of the H_2 line profiles and the response of the H_2 lines to a stellar flare, the H_2 line emission is likely produced in the star, rather than in the disk or the planet. However, the temperature of this gas is significantly below the temperature of the photosphere (∼3650 K) and the predicted temperature of its star spots ($\gtrsim$2650 K). We discuss the possibility of colder star spots or a cold layer in the photosphere of a pre-main sequence M dwarf.

22. SIRIUS Project. V. Formation of off-center ionized bubbles associated with Orion Nebula Cluster

Michiko S. Fujii, Kohei Hattori, Long Wang, Yutaka Hirai, Jun Kumamoto, Yoshito Shimajiri, Takayuki R. Saitoh ★ Massive stars born in star clusters terminate star cluster formation by ionizing the surrounding gas. This process is considered to be prevalent in young star clusters containing massive stars. The Orion Nebula is an excellent example associated with a forming star cluster including several massive stars (the Orion Nebula Cluster; ONC) and a 2-pc size HII region (ionized bubble) opening toward the observer; however, the other side is still covered with dense molecular gas. Recent astrometric data acquired by the Gaia satellite revealed the stellar kinematics in this region. By comparing this data with star cluster formation simulation results, we demonstrate that massive stars born in the ONC center were ejected via three-body encounters. Further, orbit analysis indicates that θ^2 Ori A, the second massive star in this region, was ejected from the ONC center toward the observer and is now returning to the cluster center. Such ejected massive stars can form a hole in the dense molecular cloud and contribute to the formation of the 2-pc bubble. Our results demonstrate that the dynamics of massive stars are essential for the formation of star clusters and HII regions that are not always centered by massive stars.

23. A detailed temperature map of the archetypal protostellar shocks in L1157

S. Feng, H. B. Liu, P. Caselli, A. Burkhardt, F. Du, R. Bachiller, C. Codella, C. Ceccarelli ★ We present sensitive NH_3 (1,1)–(7,7) line images from the Karl G. Jansky Very Large Array toward successive shocks, which are associated with the blueshifted outflow lobe driven by the compact protobinary system L1157. Within a projection distance of 0.1 pc, our observations not only trace the quiescent and cold gas in the flattened envelope but also illustrate the complex physical and chemical processes that take place where the high-velocity jet impinges on its surrounding medium. Specifically, the NH_3 ortho-to-para ratio is enhanced by a factor of 2–2.5 along the jet path, where the velocity offset between the line peak and the blueshifted wing reaches values as high as $10\,\mathrm{km\,s^{-1}}$; it also shows a strong spatial correlation with the NH_3 column density, which is enhanced to $> 10^{16}\,\mathrm{cm^{-2}}$ toward the shock cavities. At a linear resolution of 1500 au, our refined temperature map from the seven NH_3 lines shows a gradient from the warm B0 eastern cavity wall ($> 120\,\mathrm{K}$) to the cool cavity B1 and the earlier shock B2 ($< 80\,\mathrm{K}$), indicating shock heating.

24. Diffusion activation energy and desorption activation energy for astrochemically relevant species on water ice show no clear relation

Kenji Furuya, Tetsuya Hama, Yasuhiro Oba, Akira Kouchi, Naoki Watanabe, Yuri Aikawa ★ The activation energy for desorption (Edes) and that for surface diffusion (Esd) of adsorbed molecules on dust grains are two of the most important parameters for the chemistry in the interstellar medium. Although Edes is often measured by laboratory experiments, the measurement of Esd is sparse. Due to the lack of data, astrochemical models usually assume a simple scaling relation, Esd = fEdes, where f is a constant, irrespective of adsorbed species. Here, we experimentally measure Esd for CH4, H2S, OCS, CH3OH, and CH3CN on water-ice surfaces using an ultra-high-vacuum transmission electron microscope (UHV-TEM). Compiling the measured Esd values and Edes values from the literature, we find that the value of f ranges from 0.2 to 0.7, depending on the species. Unless f (or Esd) for the majority of species is available, a natural alternative approach for astrochemical models is running multiple simulations, varying f for each species randomly. In this approach, ranges of molecular abundances predicted by multiple simulations, rather than abundances predicted by each simulation, are important. We here run 10,000 simulations of astrochemical models of molecular clouds and protostellar envelopes, randomly assigning a value of f for each species. In the former case, we identify several key species whose Esd most strongly affects the uncertainties of the model predictions; Esd for those species should be investigated in future laboratory and quantum chemical studies. In the latter case, uncertainties in the Esd of many species contribute to the uncertainties in the model predictions.

25. Discovery of CH2CCHC4H and a rigorous detection of CH2CCHC3N in TMC-1 with the QUIJOTE line survey

R. Fuentetaja, C. Cabezas, M. Agundez, B. Tercero, N. Marcelino, J. R. Pardo, P. de Vicente, J. Cernicharo ★ Using the QUIJOTE line survey in the 32.0-50.4 GHz range, we report the discovery of the molecule CH2CCHC4H towards the prestellar cold core TMC-1 in the Taurus region. We also present a rigorous detection of CH2CCHC3N, along with its detailed analysis. We identified a total of twenty rotational transitions for each one of these molecules. The rotational quantum numbers range from Ju=17 up to 24 and Ka<=3. The column density for CH2CCHC4H is N=(2.2+/-0.2)x 1E12 cm-2, while for CH2CCHC3N, we derived N=(1.2+/-0.15) x 1E11 cm-2. The rotational temperature is 9.0+/-0.5 K for both species. The abundance ratio between CH2CCHC4H and CH2CCHC3N is 18+/-4. We also compared the column densities of these species with those of their isomers CH3C6H and CH3C5N, derived from their J=20-19 up to J=30-29 rotational transitions observed with the QUIJOTE line survey. The observed abundances for all these species are reasonably well explained by state-of-the-art chemical models of TMC-1. The observed astronomical frequencies were merged with laboratory frequencies from the literature to derive improved spectroscopic parameters.

26. Cosmic rays probed by H_2 rovibrational lines: Is chemical modeling important to understand JWST H_2 observations?

Brandt A. L. Gaches, Shmuel Bialy, Thomas G. Bisbas, Marco Padovani, Daniel Seifried, Stefanie Walch ★ Context: It has been proposed that H_2near-infrared lines may be excited by cosmic rays and allow for a determination of the cosmic-ray ionization rate in dense gas. One-dimensional models show that measuring both the H_2gas column density and H_2line intensity enables a constraint on the cosmic-ray ionization rate as well as the spectral slope of low-energy cosmic-ray protons in the interstellar medium (ISM). Aims: We aim to investigate the impact of certain assumptions regarding the H_2chemical models and ISM density distributions on the emission of cosmic-ray induced H_2emission lines. This is of particular importance for utilizing observations of these lines with the James Webb Space Telescope to constrain the cosmic-ray ionization rate. Methods: We compare the predicted emission from cosmic-ray induced, ro-vibrationally excited H_2emission lines for different one- and three-dimensional models with varying assumptions on the gas chemistry and density distribution. Results: We find that the model predictions of the H_2line intensities for the (1-0)S(0), (1-0)Q(2), (1-0)O(2) and (1-0)O(4) transitions at 2.22, 2.41, 2.63 and 3.00 μm, respectively, are relatively independent of the astro-chemical model and the gas density distribution when compared against the H_2column density, making them robust tracer of the cosmic-ray ionization rate. Conclusions: We recommend the use of ro-vibrational H_2line emission in combination with estimation of the cloud's H_2column density, to constrain the ionization rate and the spectrum of low energy cosmic-rays.

27. Formation of Dust Rings and Gaps in Non-ideal MHD Disks Through Meridional Gas Flows

Xiao Hu, Zhi-Yun Li, Zhaohuan Zhu, Chao-Chin Yang ★ Rings and gaps are commonly observed in the dust continuum emission of young stellar disks. Previous studies have shown that substructures naturally develop in the weakly ionized gas of magnetized, non-ideal MHD disks. The gas rings are expected to trap large mm/cm-sized grains through pressure gradient-induced radial dust-gas drift. Using 2D (axisymmetric) MHD simulations that include ambipolar diffusion and dust grains of three representative sizes (1 mm, 3.3 mm, and 1 cm), we show that the grains indeed tend to drift radially relative to the gas towards the centers of the gas rings, at speeds much higher than in a smooth disk because of steeper pressure gradients. However, their spatial distribution is primarily controlled by meridional gas motions, which are typically much faster than the dust-gas drift. In particular, the grains that have settled near the midplane are carried rapidly inwards by a fast accretion stream to the inner edges of the gas rings, where they are lifted up by the gas flows diverted away from the midplane by a strong poloidal magnetic field. The flow pattern in our simulation provides an attractive explanation for the meridional flows recently inferred in HD 163296 and other disks, including both "collapsing" regions where the gas near the disk surface converges towards the midplane and a disk wind. Our study highlights the prevalence of the potentially observable meridional flows associated with the gas substructure formation in non-ideal MHD disks and their crucial role in generating rings and gaps in dust.

28. Chemical and Physical Characterization of the Isolated Protostellar Source CB68: FAUST. IV

Muneaki Imai, Yoko Oya, Brian Svoboda, FAUST members ★ Chemical diversity of low-mass protostellar sources has so far been recognized, and environmental effects are invoked as its origin. In this context, observations of isolated protostellar sources without influences of nearby objects are of particular importance. Here, we report chemical and physical structures of the low-mass Class 0 protostellar source IRAS 16544−1604 in the Bok globule CB68, based on 1.3 mm ALMA observations at a spatial resolution of ∼70 au that were conducted as part of the large program FAUST. Three interstellar saturated complex organic molecules (iCOMs), CH_3OH, $HCOOCH_3$, and CH_3OCH_3, are detected toward the protostar. The rotation temperature and the emitting region size for CH_3OH are derived to be 131 ± 11 K and ∼10 au, respectively. The detection of iCOMs in close proximity to the protostar indicates that CB68 harbors a hot corino. The kinematic structure of the $C^{18}O$, CH_3OH, and OCS

lines is explained by an infalling-rotating envelope model, and the protostellar mass and the radius of the centrifugal barrier are estimated to be $0.08 - 0.30\ M_{\odot}$ and < 30 au, respectively. The small radius of the centrifugal barrier seems to be related to the small emitting region of iCOMs. In addition, we detect emission lines of c-C_3H_2 and CCH associated with the protostar, revealing a warm carbon chain chemistry (WCCC) on a 1000 au scale. We therefore find that the chemical structure of CB68 is described by a hybrid chemistry. The molecular abundances are discussed in comparison with those in other hot corino sources and reported chemical models.

29. Star Formation Activity Beyond the Outer Arm II: Distribution and Properties of Star Formation

Natsuko Izumi, Naoto Kobayashi, Chikako Yasui, Masao Saito, Satoshi Hamano, Patrick M. Koch ★ The outer Galaxy beyond the Outer Arm represents a promising opportunity to study star formation in an environment vastly different from the solar neighborhood. In our previous study, we identified 788 candidate star-forming regions in the outer Galaxy (at galactocentric radii $R_{\rm G} \geq 13.5$ kpc) based on Wide-field Infrared Survey Explorer (WISE) mid-infrared (MIR) all-sky survey. In this paper, we investigate the statistical properties of the candidates and their parental molecular clouds derived from the Five College Radio Astronomy Observatory (FCRAO) CO survey. We show that the molecular clouds with candidates have a shallower slope of cloud mass function, a larger fraction of clouds bound by self-gravity, and a larger density than the molecular clouds without candidates. To investigate the star formation efficiency (SFE) at different $R_{\rm G}$, we used two parameters: 1) the fraction of molecular clouds with candidates and 2) the monochromatic MIR luminosities of candidates per parental molecular cloud mass. We did not find any clear correlation between SFE parameters and $R_{\rm G}$ at $R_{\rm G}$ of 13.5 kpc to 20.0 kpc, suggesting that the SFE is independent of environmental parameters such as metallicity and gas surface density, which vary considerably with $R_{\rm G}$. Previous studies reported that the SFE per year (SFE/yr) derived from the star-formation rate surface density per total gas surface density, HI plus H_2, decreases with increased $R_{\rm G}$. Our results might suggest that the decreasing trend is due to a decrease in HI gas conversion to H_2 gas.

30. Statistical properties and correlation length in star-forming molecular clouds: I. Formalism and application to observations

Etienne Jaupart, Gilles Chabrier ★ The proper characterization of the general statistical behavior of these fluctuations, from a limited sample of observations or simulations, is of prime importance to understand the process of star formation. In this article, we use the ergodic theory for any random field of fluctuations, as commonly used in statistical physics, to derive rigorous statistical results. We outline how to evaluate the autocovariance function (ACF) and the characteristic correlation length of these fluctuations. We then apply this statistical approach to astrophysical systems characterized by a field of density fluctuations, notably star-forming clouds. When it is difficult to determine the correlation length from the empirical ACF, we show alternative ways to estimate the correlation length. We show that the statistics of the column-density field is hampered by biases introduced by integration effects along the line of sight and we explain how to reduce these biases. The statistics of the probability density function (PDF) ergodic estimator also yields the derivation of the proper statistical error bars. We provide a method that can be used by observers and numerical simulation specialists to determine the latter. We show that they (i) cannot be derived from simple Poisson statistics and (ii) become increasingly large for increasing density contrasts, severely hampering the accuracy of the low and high end part of the PDF because of a sample size that is too small. As templates of various stages of star formation in MCs, we then examine the case of the Polaris and Orion B clouds in detail. We calculate, from the observations, the ACF and the correlation length in these clouds and show that the latter is on the order of $\sim$1% of the size of the cloud.

31. Statistical properties and correlation length in star-forming molecular clouds: II. Gravitational potential and virial parameter

Etienne Jaupart, Gilles Chabrier ★ In the first article of this series, we have used the ergodic theory to assess the validity of a statistical approach to characterize various properties of star-forming molecular clouds (MCs) from a limited number of observations or simulations. This allows the proper determination of confidence intervals for various volumetric averages of statistical quantities obtained form observations or numerical simulations. In this joint paper, we apply the same formalism to a different kind of (observational or numerical) study of MCs. Indeed, as observations cannot fully unravel the complexity of the inner density structure of star forming clouds, it is important to know whether global observable estimates, such as the total mass and size of the cloud, can give an accurate estimation of various key physical quantities that characterize the dynamics of the cloud. Of prime importance is the correct determination of the total gravitational (binding) energy and virial parameter of a cloud. We show that, whereas for clouds that are not in a too advanced stage of star formation, such as Polaris or Orion B, the knowledge of only their mass and size is sufficient to yield an accurate determination of the aforementioned quantities from observations (i.e. in real space). In contrast, we show that this is no longer true for numerical simulations in a periodic box. We derive a relationship for the ratio of the virial parameter in these two respective cases.

32. Super-resolution trends in the ALMA Taurus survey: Structured inner discs and compact discs

Jeff Jennings, Marco Tazzari, Cathie J. Clarke, Richard A. Booth, Giovanni P. Rosotti ★ The 1.33 mm survey of protoplanetary discs in the Taurus molecular cloud found annular gaps and rings to be common in extended sources (> 55 au), when their 1D visibility distributions were fit parametrically. We first demonstrate the advantages and limitations of nonparametric visibility fits for data at the survey's 0.12" resolution. Then we use the nonparametric model in Frankenstein ('frank') to identify new substructure in three compact and seven extended sources. Among the new features we identify three trends: a higher occurrence rate of substructure in the survey's compact discs than previously seen, underresolved (potentially azimuthally asymmetric) substructure in the innermost disc of extended sources, and a 'shoulder' on the trailing edge of a ring in discs with strong depletion at small radii. Noting the shoulder morphology is present in multiple discs observed at higher resolution, we postulate it is tracing a common physical mechanism. We further demonstrate how a super-resolution frank brightness profile is useful in motivating an accurate parametric model, using the highly structured source DL Tau in which frank finds two new rings. Finally we show that sparse (u, v) plane sampling may be masking the presence of substructure in several additional compact survey sources.

33. A multiwavelength study of the W33 Main ultracompact HII region

Sarwar Khan, Jagadheep D. Pandian, Dharam V. Lal, Michael R. Rugel, Andreas Brunthaler, Karl M. Menten, F. Wyrowski, S-N. X. Medina, S. A. Dzib, H. Nguyen ★ The dynamics of ionized gas around the W33 Main ultracompact HII region is studied using observations of hydrogen radio recombination lines and a detailed multiwavelength characterization of the massive star-forming region W33 Main is performed. We used the Giant Meterwave Radio Telescope (GMRT) to observe the H167α recombination line at 1.4 GHz at an angular resolution of 10 arcsec, and Karl. G. Jansky Very Large Array (VLA) data acquired in the GLOSTAR survey to study the dynamics of ionized gas. We also observed the radio continuum at 1.4 GHz and 610 MHz with the GMRT and used GLOSTAR 4−8 GHz continuum data to characterize the nature of the radio emission. In addition, archival data from submillimeter to near-infrared wavelengths were used to study the dust emission and identify YSOs in the W33 Main star-forming region. The radio recombination lines were detected at good signal to noise in the GLOSTAR data, while the H167α radio recombination line was marginally detected with the GMRT. The spectral index of radio emission in the region determined from GMRT and GLOSTAR shows the emission to be thermal in the entire region. Along with W33 Main, an arc-shaped diffuse continuum source, G12.81−0.22, was detected with the GMRT data. The GLOSTAR recombination line data reveal a velocity gradient across W33 Main and G12.81−0.22. The electron temperature is found to be 6343 K and 4843 K in W33 Main and G12.81−0.22, respectively. The physical properties of the W33 Main molecular clump were derived by modeling the dust emission using data from the ATLASGAL and Hi-GAL surveys and they are consistent with the region being a relatively evolved site of massive star formation. The gas dynamics and physical properties of G12.81−0.22 are consistent with the HII region being in an evolved phase and its expansion on account of the pressure difference is slowing down.

34. The morphology of CSCha circumbinary disk suggesting the existence of a Saturn-mass planet

N. T. Kurtovic, P. Pinilla, Anna B. T. Penzlin, M. Benisty, L. Pérez, C. Ginski, A. Isella, W. Kley, F. Menard, S. Pérez, A. Bayo ★ Planets have been detected in circumbinary orbits in several different systems, despite the additional challenges faced during their formation in such an environment. We investigate the possibility of planetary formation in the spectroscopic binary CS Cha by analyzing its circumbinary disk. The system was studied with high angular resolution ALMA observations at 0.87mm. Visibilities modeling and Keplerian fitting are used to constrain the physical properties of CS Cha, and the observations were compared to hydrodynamic simulations. Our observations are able to resolve the disk cavity in the dust continuum emission and the 12CO J:3-2 transition. We find the dust continuum disk to be azimuthally axisymmetric (less than 9% of intensity variation along the ring) and of low eccentricity (of 0.039 at the peak brightness of the ring). Under certain conditions, low eccentricities can be achieved in simulated disks without the need of a planet, however, the combination of low eccentricity and axisymmetry is consistent with the presence of a Saturn-like planet orbiting near the edge of the cavity.

35. Dynamical star forming history of Per OB2

Marina Kounkel, TingYan Deng, Keivan G. Stassun ★ We analyze the internal dynamics of young stars towards Perseus using Gaia EDR3 data, including Per OB2 and California Cloud. Interpreting the current dynamics, we speculate that Per OB2 may have formed from two separate clouds that have begun forming stars in a close proximity of each other. IC 348 is caught in the middle between the two of them, inheriting kinematics of both, and it stands out as a possible site of cloud cloud interaction. We also consider a possibility of a past supernova in Per OB2 - while one had likely occurred, it did not appear to have caused any obvious triggered star formation, but it has created a shock which has swept away the molecular gas away from IC 348. Finally, we examine a recently proposed shell between Taurus and Perseus. While its origin is unknown, we find no support for an expanding bubble in stellar kinematics, nor can we identify a likely progenitor for a supernova that may have

caused it, disfavoring this scenario in the formation of this apparent shell.

36. The Role of Magnetic Fields in the Stability and Fragmentation of Filamentary Molecular Clouds: Two Case Studies at OMC-3 and OMC-4

Pak Shing Li, Enrique Lopez-Rodriguez, Archana Soam, Richard I. Klein ★ We present the stability analysis of two regions, OMC-3 and OMC-4, in the massive and long molecular cloud complex of Orion A. We obtained 214 μm HAWC+/SOFIA polarization data, and we make use of archival data for the column density and $C^{18}O$ (1-0) emission line. We find clear depolarization in both observed regions and that the polarization fraction is anti-correlated with the column density and the polarization-angle dispersion function. We find that the filamentary cloud and dense clumps in OMC-3 are magnetically supercritical and strongly subvirial. This region should be in the gravitational collapse phase and is consistent with many young stellar objects (YSOs) forming in the region. Our histogram of relative orientations (HROs) analysis shows that the magnetic field is dynamically sub-dominant in the dense gas structures of OMC-3. We present the first polarization map of OMC-4. We find that the observed region is generally magnetically subcritical except for an elongated dense core, which could be a result of projection effect of a filamentary structure aligned close to the line-of-sight. The relative large velocity dispersion and the unusual positive shape parameters at high column densities in the HROs analysis suggest that our viewing angle may be close to axes of filamentary substructures in OMC-4. The dominating strong magnetic field in OMC-4 is unfavorable for star formation and is consistent with much fewer YSOs than in OMC-3.

37. A massive Keplerian protostellar disk with flyby-induced spirals in the Central Molecular Zone

Xing Lu, Guang-Xing Li, Qizhou Zhang, Yuxin Lin ★ Accretion disks are an essential component in the paradigm of the formation of low-mass stars. Recent observations further identify disks surrounding low-mass pre-main-sequence stars perturbed by flybys. Whether disks around more massive stars evolve in a similar manner becomes an urgent question. We report the discovery of a Keplerian disk of a few solar masses surrounding a 32 solar-mass protostar in the Sagittarius C cloud around the Galactic Center. The disk is gravitationally stable with two embedded spirals. A combined analysis of analytical solutions and numerical simulations demonstrates that the most likely scenario to form the spirals is through external perturbations induced by a close flyby, and one such perturber with the expected parameters is identified. The massive, early O-type star embedded in this disk forms in a similar manner with respect to low-mass stars, in the sense of not only disk-mediated accretion, but also flyby-impacted disk evolution.

38. Gaia EDR3 comparative study of protoplanetary disk fractions in young stellar clusters

I. Mendigutía, E. Solano, M. Vioque, L. Balaguer-Nuñez, A. Ribas, N. Huélamo, C. Rodrigo ★ (Abridged) The lifetime of protoplanetary disks around young stars limits the timescale when planets form. A disk dissipation timescale < 10 Myr was inferred from surveys providing the fraction of stars with disks in young stellar clusters with different ages. However, most previous surveys focused on the compact region within 2 pc from the clusters' centers, for which the disk fraction information considering the outer part is practically absent. We aim to test if disk fraction estimates change when inferred from an extended region around the clusters' centers. Gaia EDR3 data and a best-suited, Virtual Observatory (VO)-based tool -Clusterix-, are used to identify member stars for a representative sample of 19 young clusters considering two concentric fields of view (FOV) with radii 20 pc and 2 pc. Our analysis reveals that the inner disk fractions inferred from the compact and the extended regions are equal within 10%, which does not support a previous hypothesis proposing that disk fractions should be significantly larger considering extended regions. A list of member and disk stars in each cluster is provided and stored in a VO-compliant archive. Averaged values and plots characterizing the whole clusters are also provided, including HR diagrams based on Gaia colors and absolute magnitudes. Our results cover the largest fields ever probed when dealing with disk fractions for all clusters analysed, and imply that their complete characterization requires the use of wide FOVs. The resulting database is a benchmark for future detailed studies of young clusters, whose disk fractions must be accurately determined by using multi-wavelength analysis potentially combined with data from coming Gaia releases.

39. Gas Column Density Distribution of Molecular Clouds in the Third Quadrant of the Milky Way

Yuehui Ma, Hongchi Wang, Miaomiao Zhang, Chen Wang, Shaobo Zhang, Yao Liu, Chong Li, Yuqing Zheng, Lixia Yuan, Ji Yang ★ We have obtained column density maps for an unbiased sample of 120 molecular clouds in the third quadrant of the Milky Way mid-plane ($b \leq |5|^\circ$) within the galactic longitude range from 195° to 225°, using the high sensitivity ^{12}CO and ^{13}CO ($J = 1 - 0$) data from the Milky Way Imaging Scroll Painting (MWISP) project. The probability density functions of the molecular hydrogen column density of the clouds, N-PDFs, are fitted with both log-normal (LN) function and log-normal plus power-law (LN+PL) function. The molecular clouds are classified into three categories according to their shapes of N-PDFs, i.e., LN, LN+PL, and UN (unclear), respectively. About 72% of the molecular clouds fall into the LN category,

while 18% and 10% into the LN+PL and UN categories, respectively. A power-law scaling relation, $\sigma_s \propto N_{H_2}^{0.44}$, exists between the width of the N-PDF, σ_s, and the average column density, N_{H_2}, of the molecular clouds. However, σ_s shows no correlation with the mass of the clouds. A correlation is found between the dispersion of normalized column density, $\sigma_{N/<N>}$, and the sonic Mach number, $\mathcal{M}$, of molecular clouds. Overall, as predicted by numerical simulations, the N-PDFs of the molecular clouds with active star formation activity tend to have N-PDFs with power-law high-density tails.

40. Modeling snowline locations in protostars: The impact of the structure of protostellar cloud cores

Nadia M. Murillo, Tien-Hao Hsieh, Catherine Walsh ★ Abridged Context: Snowlines during star and disk formation are responsible for a range of effects during the evolution of protostars, such as setting the chemical composition of the envelope and disk. This in turn influences the formation of planets by changing the elemental compositions of solids and affecting the collisional properties and outcomes of dust grains. Snowlines can also reveal accretion bursts, providing insight into the formation process of stars. Methods: A numerical chemical network coupled with a grid of cylindrical-symmetric physical models was used to identify what physical parameters alter the CO and H_2O snowline locations. The investigated parameters are the initial molecular abundances, binding energies of CO and H_2O, heating source, cloud core density, outflow cavity opening angle, and disk geometry. Simulated molecular line emission maps were used to quantify the change in the snowline location with each parameter. Conclusions: The models presented in this work show that the CO and H_2O snowline locations do not occur at a single, well-defined temperature as is commonly assumed. Instead, the snowline position depends on luminosity, cloud core density, and whether a disk is present or not. Inclination and spatial resolution affect the observability and successful measurement of snowline locations. We note that N_2H^+ and HCO^+ emission serve as good observational tracers of CO and H_2O snowline locations. However, constraints on whether or not a disk is present, the observation of additional molecular tracers, and estimating envelope density will help in accurately determining the cause of the observed snowline position. Plots of the N_2H^+ and HCO^+ peak emission radius versus luminosity are provided to compare the models with observations of deeply embedded protostars aiming to measure the CO and H_2O snowline locations.

41. ALMA Images the Eccentric HD 53143 Debris Disk

Meredith A. MacGregor, Spencer A. Hurt, Christopher C. Stark, Ward S. Howard, Alycia J. Weinberger, Bin Ren, Glenn Schneider, Elodie Choquet, Dmitri Mawet ★ We present ALMA 1.3 mm observations of the HD 53143 debris disk - the first infrared or millimeter image produced of this 1 Gyr-old solar-analogue. Previous HST STIS coronagraphic imaging did not detect flux along the minor axis of the disk which could suggest a face-on geometry with two 'clumps' of dust. These ALMA observations reveal a disk with a strikingly different structure. In order to fit models to the millimeter visibilities and constrain the uncertainties on the disk parameters, we adopt an MCMC approach. This is the most eccentric debris disk observed to date with a forced eccentricity of 0.21 ± 0.02, nearly twice that of the Fomalhaut debris disk, and also displays apocenter glow. Although this eccentric model fits the outer debris disk well, there are significant interior residuals remaining that may suggest a possible edge-on inner disk, which remains unresolved in these observations. Combined with the observed structure difference between HST and ALMA, these results suggest a potential previous scattering event or dynamical instability in this system. We also note that the stellar flux changes considerably over the course of our observations, suggesting flaring at millimeter wavelengths. Using simultaneous TESS observations, we determine the stellar rotation period to be 9.6 ± 0.1 days.

42. Unraveling the observational signatures of cloud-cloud collision and hub-filament systems in W31

A. K. Maity, L. K. Dewangan, H. Sano, K. Tachihara, Y. Fukui, N. K. Bhadari ★ To understand the formation process of massive stars, we present a multi-scale and multi-wavelength study of the W31 complex hosting two extended HII regions (i.e., G10.30-0.15 (hereafter, W31-N) and G10.15-0.34 (hereafter, W31-S)) powered by a cluster of O-type stars. Several Class I protostars and a total of 49 ATLASGAL 870 μm dust clumps (at d = 3.55 kpc) are found toward the HII regions where some of the clumps are associated with the molecular outflow activity. These results confirm the existence of a single physical system hosting the early phases of star formation. The Herschel 250 μm continuum map shows the presence of hub-filament system (HFS) toward both W31-N and W31-S. The central hubs harbour HII regions and they are depicted with extended structures (with $T_d \sim$ 25-32 K) in the Herschel temperature map. In the direction of W31-S, an analysis of the NANTEN2 ^{12}CO(J = 1-0) and SEDIGISM ^{13}CO(J = 2-1) line data supports the presence of two cloud components around 8 and 16 km s^{-1}, and their connection in velocity space. A spatial complementary distribution between the two cloud components is also investigated toward W31-S, where the signposts of star formation, including massive O-type stars, are concentrated. These findings favor the applicability of cloud-cloud collision (CCC) around ~2 Myr ago in W31-S. Overall, our observational findings support the theoretical scenario of CCC in W31, which explains the formation of massive stars and the existence of HFSs.

43. The halo around HD 32297: μm-sized cometary dust

Johan Olofsson, Philippe Thébault, Grant M. Kennedy, Amelia Bayo ★ The optical properties of the second generation dust that we observe in debris disks remain quite elusive, whether it is the absorption efficiencies at millimeter wavelengths or the (un)polarized phase function at near-infrared wavelengths. Thankfully the same particles are experiencing forces that are size dependent (e.g., radiation pressure), and with high angular resolution observations we can take advantage of this natural spatial segregation. Observations at different wavelengths probe different ranges of sizes, and there is therefore a great synergy in multi-wavelength observations to better constrain the optical properties of the particles. We present a new approach to simultaneously model SPHERE and ALMA observations and apply it to the debris disk around HD 32297, putting the emphasis on the spatial distribution of the grains with different β values. This modeling approach requires few assumptions on the actual sizes of the particles and the interpretation can therefore be done a posteriori. We find that the ALMA observations are best reproduced with a combination of small and large β values (0.03 and 0.42) while the SPHERE observations require several intervals of β values. We discuss the nature of the halo previously reported in ALMA observations, and hypothesize it could be caused by over-abundant μm-sized particles (the over-abundance being the consequence of their extended lifetime). We model the polarized phase function at near-infrared wavelengths and fluffy aggregates larger than a few μm provide the best solution. Comparing our results with comets of the solar system, we postulate that the particles released in the disk originate from rather pristine cometary bodies (to avoid compaction of the fluffy aggregates) and are then set on highly eccentric orbits, which could explain the halo detected at long wavelengths.

44. Formation of dust clumps with sub-Jupiter mass and cold shadowed region in gravitationally unstable disk around Class 0/I protostar in L1527 IRS

Satoshi Ohashi, Riouhei Nakatani, Hauyu Baobab Liu, Hiroshi Kobayashi, Yichen Zhang, Tomoyuki Hanawa, Nami Sakai ★ We have investigated the protostellar disk around a Class 0/I protostar, L1527 IRS, using multi-wavelength observations of the dust continuum emission at λ = 0.87, 2.1, 3.3, and 6.8 mm obtained by the Atacama Large Millimeter/submillimeter Array (ALMA) and the Jansky Very Large Array (VLA). Our observations achieved a spatial resolution of $3-13$ au and revealed an edge-on disk structure with a size of $\sim 80-100$ au. The emission at 0.87 and 2.1 mm is found to be optically thick within a projected disk radius of $r_{\rm proj} \lesssim 50$ au. The emission at 3.3 and 6.8 mm shows that the power-law index of the dust opacity (β) is $\beta \sim 1.7$ around $r_{\rm proj} \sim 50$ au, suggesting that grain growth has not yet begun. The dust temperature ($T_{\rm dust}$) shows a steep decrease with $T_{\rm dust} \propto r_{\rm proj}^{-2}$ outside of the VLA clumps previously identified at $r_{\rm proj} \sim 20$ au. Furthermore, the disk is gravitationally unstable at $r_{\rm proj} \sim 20$ au, as indicated by a Toomre Q parameter value of $Q \lesssim 1.0$. These results suggest that the VLA clumps are formed via gravitational instability, which creates a shadow on the outside of the substructure, resulting in the sudden drop in temperature. The derived dust masses for the VLA clumps are $\gtrsim 0.1$ $M_{\rm J}$. Thus, we suggest that Class 0/I disks can be massive enough to be gravitationally unstable, which might be the origin of gas-giant planets in a 20 au radius. Furthermore, the protostellar disks can be cold due to shadowing.

45. No evidence of the significant grain growth but tentative discovery of disk substructure in a disk around the Class I Protostar L1489 IRS

Satoshi Ohashi, Hiroshi Kobayashi, Jinshi Sai, Nami Sakai ★ For revealing the first step of the plant formation, it is important to understand how and when dust grains become larger in a disk around a protostar. To investigate the grain growth, we analyze dust continuum emission toward a disk around the Class I protostar, L1489 IRS at 0.9 and 1.3 mm wavelengths obtained by the Atacama Large Millimeter/submillimeter Array. The dust continuum emission extends to a disk radius (r) of $r \sim 300$ au, and the spectral index (α) is derived to be $\alpha \sim 3.6$ at a radius of $r \sim 100-300$ au, as similar to the interstellar dust. Therefore, the grain growth does not occur significantly in the outer disk ($r \sim 100-300$ au). Furthermore, we tentatively identify a ring-like substructure at $r \sim 90$ au even though the spatial resolution and sensitivity are not enough to determine this structure. If this is the real ring structure, the ring position and small dust in the disk outer part are consistent with the idea of the growth front. These results suggest that the L1489 protostellar disk may be the beginning of the planet formation.

46. The Effects of Cosmic Rays on the Chemistry of Dense Cores

Ross O'Donoghue, Serena Viti, Marco Padovani, Tomas James ★ Cosmic rays are crucial for the chemistry of molecular clouds and their evolution. They provide essential ionizations, dissociations, heating and energy to the cold, dense cores. As cosmic rays pierce through the clouds they are attenuated and lose energy, which leads to a dependency on the column density of a system. The detailed effects these particles have on the central regions still needs to be fully understood. Here, we revisit how cosmic rays are treated in the UCLCHEM chemical modeling code by including both ionization rate and H2 dissociation rate dependencies alongside the production of cosmic ray induced excited species and we study in detail the effects of these treatments on the chemistry of pre-stellar cores. We find that these treatments can have significant effects on chemical abundances, up to several orders of magnitude, depending on physical conditions. The ionization dependency is the most significant treatment, influencing chemical abundances through increased presence of ionized species, grain desorptions and enhanced chemical reactions. Comparisons to chemical abundances derived from observations show the new treatments

reproduce these observations better than the standard handling. It is clear that more advanced treatments of cosmic rays are essential to chemical models and that including this type of dependency provides more accurate chemical representations.

47. Low mass young stars in the Milky Way unveiled by DBSCAN and Gaia EDR3. Mapping the star forming regions within 1.5 Kpc

L. Prisinzano, F. Damiani, S. Sciortino, E. Flaccomio, M. G. Guarcello, G. Micela, E. Tognelli, R. D. Jeffries, J. M. Alcalá ★ With an unprecedented astrometric and photometric data precision, Gaia EDR3 gives us, for the first time, the opportunity to systematically detect and map in the optical bands, the low mass populations of the star forming regions (SFRs) in the Milky Way. We provide a catalogue of the Gaia EDR3 data (photometry, proper motions and parallaxes) of the young stellar objects (YSOs) identified in the Galactic Plane (|b|<30 deg) within about 1.5 kpc. The catalogue of the SFRs to which they belong is also provided to study the properties of the very young clusters and put them in the context of the Galaxy structure. We applied the machine learning unsupervised clustering algorithm DBSCAN on a sample of Gaia EDR3 data photometrically selected on the region where very young stars (t<10 Myr) are expected to be found, with the aim to identify co-moving and spatially consistent stellar clusters. A subsample of 52 clusters, selected among the 7323 found with DBSCAN, has been used as template data set, to identify very young clusters from the pattern of the observed color-absolute magnitude diagrams through a pattern match process. We find 124440 candidate YSOs clustered in 354 SFRs and stellar clusters younger than 10 Myr and within about 1.5 Kpc. In addition, 65863 low mass members of 322 stellar clusters located within about 500 pc and with ages 10 Myr<t<100 Myr were also found. The selected YSOs are spatially correlated with the well known SFRs. Most of them are associated with well concentrated regions or complex structures of the Galaxy and a substantial number of them have been recognized for the first time. The massive SFRs, such as, for example, Orion, Sco-Cen and Vela, located within 600-700 pc trace a very complex three-dimensional pattern, while the farthest ones seem to follow a more regular pattern along the Galactic Plane.

48. Efficient Dust Radial Drift Around Young Intermediate-mass Stars

Paola Pinilla, Antonio Garufi, Matías Gárate ★ The radial velocities and direct imaging observations of exoplanets have suggested that the frequency of giant planets may decrease for intermediate-mass stars ($2.5-8\,M_{\odot}$). The key mechanism that could hinder their formation remains unclear. From a theoretical point of view, planet formation around intermediate-mass stars may take place on longer timescales, which – coupled with fast migration and efficient photoevaporation – may prevent planetary formation in these environments. In this letter, we investigate the temporal evolution of the radial drift for dust particles in disks when stellar evolution is taken into account. We demonstrate that the particle drift velocity around intermediate-mass stars sharply increases after 1−2 Myr, potentially forming a difficult barrier to overcome in the first steps of planet formation. This high radial drift could explain the lack of disk detections around intermediate-mass stars older than 3−4 Myr, as opposed to low-mass stars ($< 2.5\,M_{\odot}$), where the drift may not be the most impactful factor for the disk evolution. Future high-resolution images of these disks can help us to explain why planets around intermediate-mass stars may be rare. In addition, we can explore whether the role of efficient dust radial drift does in fact hinder planet formation around intermediate-mass stars – or otherwise.

49. The Distributions of Gas, Small-, and Large-grains in the LkHα 330, Disk Trace a Young Planetary System

P. Pinilla, M. Benisty, N. T. Kurtovic, J. Bae, R. Dong, Z. Zhu, S. Andrews, J. Carpenter, C. Ginski, J. Huang, A. Isella, L. Pérez, L. Ricci, G. Rosotti, M. Villenave, D. Wilner ★ [abridged] We present new scattered light and millimeter observations of the protoplanetary disk around LkHα 330, using SPHERE/VLT and ALMA respectively. The scattered-light SPHERE observations reveal an asymmetric ring at around 45 au distance from the star in addition to two spiral arms with similar radial launching points at around 90 au. The millimeter observations from ALMA (resolution of 0.06"×0.04") show mainly an asymmetric ring located at 110 au distance from the star. In addition to this asymmetry, there are two faint symmetric rings at 60 au and 200 au. The ^{12}CO, ^{13}CO and C^{18}O lines seem to be less abundant in the inner disk (these observations have a resolution of 0.16"×0.11"). The ^{13}CO peaks at a location similar to the inner ring observed with SPHERE, suggesting that this line is optically thick and traces variations of disk temperature instead of gas surface density variations, while the C^{18}O peaks slightly further away at around 60 au. We compare our observations with hydrodynamical simulations that include gas and dust evolution, and conclude that a 10 $M_{\rm Jup}$ mass planet at 60 au and in an eccentric orbit ($e = 0.1$) can qualitatively explain most of the observed structures. A planet in a circular orbit leads to a much narrower concentration in the millimeter emission, while a planet in a more eccentric orbit leads to a very eccentric cavity as well. In addition, the outer spiral arm launched by the planet changes its pitch angle along the spiral due to the eccentricity and when it interacts with the vortex, potentially appearing in observations as two distinct spirals. Our observations and models show that LkHα 330, is an exciting target to search for (eccentric-) planets while they are still embedded in their parental disk, making it an excellent candidate for studies on planet-disk interaction.

50. Large-scale expansion of OB stars in Cygnus

Alexis L. Quintana, Nicholas J. Wright ★ The proper motions (PMs) of OB stars in Cygnus have recently been found to exhibit two large-scale kinematic patterns suggestive of expansion. We perform a 3D traceback on these OB stars, the newly-identified OB associations and related open clusters in the region. We find that there are two groups of stars, associations and clusters and that they were each more compact in the past, reaching their closest approach $7.9^{+3.0}_{-1.8}$ and $8.5^{+0.8}_{-2.8}$ Myr ago. We consider two main scenarios for the driver of these large-scale expansion patterns: feedback-driven expansion from a previous generation of massive stars, and expansion as a result of the turbulent velocity field in the primordial molecular cloud. While it is tempting to attribute such large-scale expansion patterns to feedback processes, we find that the observed kinematics are fully consistent with the turbulent origin, and therefore that the injection of further energy or momentum from feedback is not required. Similar conclusions may be drawn for other star forming regions with large-scale expansion patterns.

51. Molecular precursors of the RNA-world in space: new nitriles in the G+0.693-0.027 molecular cloud

Víctor M. Rivilla, Izaskun Jiménez-Serra, Jesus Martín-Pintado, Laura Colzi, Belén Tercero, Pablo de Vicente, Shaoshan Zeng, Sergio Martín, Juan García de la Concepción, Luca Bizzocchi, Mattia Melosso, Fernando Rico-Villas, Miguel A. Requena-Torres ★ Nitriles play a key role as molecular precursors in prebiotic experiments based on the RNA-world scenario for the origin of life. These chemical compounds could have been partially delivered to the young Earth from extraterrestrial objects, stressing the importance of establishing the reservoir of nitriles in the interstellar medium. We report here the detection towards the molecular cloud G+0.693-0.027 of several nitriles, including cyanic acid (HOCN), and three C_4H_3N isomers (cyanoallene, CH_2CCHCN; propargyl cyanide, $HCCCH_2CN$; and cyanopropyne (CH_3CCCN), and the tentative detections of cyanoformaldehyde (HCOCN), and glycolonitrile ($HOCH_2CN$). We have also performed the first interstellar search of cyanoacetaldehyde ($HCOCH_2CN$), which was not detected. Based on the derived molecular abundances of the different nitriles in G+0.693-0.027 and other interstellar sources, we have discussed their formation mechanisms in the ISM. We propose that the observed HOCN abundance in G+0.693-0.027 is mainly due to surface chemistry and subsequent shock-induced desorption, while HCOCN might be mainly formed through gas-phase chemistry. In the case of $HOCH_2CN$, several grain-surface routes from abundant precursors could produce it. The derived abundances of the three C_4H_3N isomers in G+0.693-0.027 are very similar, and also similar to those previously reported in the dark cold cloud TMC-1. This suggests that the three isomers are likely formed through gas-phase chemistry from common precursors, possibly unsaturated hydrocarbons (CH_3CCH and CH_2CCH_2) that react with the cyanide radical (CN). The rich nitrile feedstock found towards G+0.693-0.027 confirms that interstellar chemistry is able to synthesize in space molecular species that could drive the prebiotic chemistry of the RNA-world.

52. Turbulent magnetic field in the HII region Sh 2-27

N. C. Raycheva, M. Haverkorn, S. Ideguchi, J. M. Stil, B. M. Gaensler, X. Sun, J. L. Han, E. Carretti, X. Y. Gao, T. Wijte ★ Magnetic fields in the turbulent interstellar medium (ISM) are a key element in understanding Galactic dynamics, but there are many observational challenges. One useful probe for studying the magnetic field component parallel to the line of sight (LoS) is Faraday rotation of linearly polarized radio synchrotron emission, combined with Hα observations. HII regions are the perfect laboratories to probe such magnetic fields as they are localized in space, and are well-defined sources often with known distances and measurable electron densities. We chose the HII region Sharpless 2-27 (Sh 2-27). By using a map of the magnetic field strength along the LoS ($B_\parallel$) for the first time, we investigate the basic statistical properties of the turbulent magnetic field inside Sh 2-27. We study the scaling of the magnetic field fluctuations, compare it to the Kolmogorov scaling, and attempt to find an outer scale of the turbulent magnetic field fluctuations. We estimate the median value of n_e as 7.3 ± 0.1 cm^{-3}, and the median value of $B_\parallel$ as -4.5 ± 0.1 μG, which is comparable to the magnetic field strength in diffuse ISM. The slope of the structure function of the estimated $B_\parallel$-map is found to be slightly steeper than Kolmogorov, consistent with our Gaussian-random-field $B_\parallel$ simulations revealing that an input Kolmogorov slope in the magnetic field results in a somewhat steeper slope in $B_\parallel$. These results suggest that the lower limit to the outer scale of turbulence is 10 pc in the HII region, which is comparable to the size of the computation domain. This may indicate that the turbulence probed here could actually be cascading from the larger scales in the ambient medium, associated with the interstellar turbulence in the general ISM, which is illuminated by the presence of Sh 2-27.

53. A survey of HDCO and D_2CO towards Class 0/I proto-brown dwarfs

B. Riaz, W. -F. Thi ★ Deuterium fractionation can constrain the physical and chemical conditions at the early stage of brown dwarf formation. We present IRAM 30m observations over a wide frequency range of 213-279 GHz of singly and doubly deuterated species of formaldehyde (HDCO and D_2CO) towards Class 0/I proto-brown dwarfs (proto-BDs). Multiple low-excitation HDCO and D_2CO transition lines with upper energy level $\leq$ 40 K are detected. The D_2CO/HDCO, HDCO/H_2CO, D_2CO/H_2CO abundance ratios range between 0.01 and 2.5 for the proto-BDs, similar to the range seen in low-mass protostars. The highest ratios of D_2CO/HDCO $\sim$1.3-2.5 are measured for two Stage 0 proto-BDs. These objects could possess a warm

corino, similar to the few hot corino cases reported among Class 0 protostars. The mean $D_2CO/HDCO$, D_2CO/H_2CO, and $HDCO/H_2CO$ ratios for the proto-BDs are comparatively higher than the range predicted by the current gas-grain chemical models, indicating that HDCO and D_2CO are formed via grain surface reactions in the dense and cold interiors of the proto-BDs at an early formation stage.

54. Gemini-LIGHTS: Herbig Ae/Be and massive T-Tauri protoplanetary disks imaged with Gemini Planet Imager

Evan A. Rich, John D. Monnier, Alicia Aarnio, Anna S. E. Laws, Benjamin R. Setterholm, David J. Wilner, Nuria Calvet, Tim Harries, Chris Miller, Claire L. Davies, Fred C. Adams, Sean M. Andrews, Jaehan Bae, Catherine Espaillat, Alexandra Z. Greenbaum, Sasha Hinkley, Stefan Kraus, Lee Hartmann, Andrea Isella, Melissa McClure, Rebecca Oppenheimer, Laura M. Pérez, Zhaohuan Zhu ★ We present the complete sample of protoplanetary disks from the Gemini- Large Imaging with GPI Herbig/T-tauri Survey (Gemini-LIGHTS) which observed bright Herbig Ae/Be stars and T-Tauri stars in near-infrared polarized light to search for signatures of disk evolution and ongoing planet formation. The 44 targets were chosen based on their near- and mid-infrared colors, with roughly equal numbers of transitional, pre-transitional, and full disks. Our approach explicitly did not favor well-known, "famous" disks or those observed by ALMA, resulting in a less-biased sample suitable to probe the major stages of disk evolution during planet formation. Our optimized data reduction allowed polarized flux as low as 0.002% of the stellar light to be detected, and we report polarized scattered light around 80% of our targets. We detected point-like companions for 47% of the targets, including 3 brown dwarfs (2 confirmed, 1 new), and a new super-Jupiter mass candidate around V1295 Aql. We searched for correlations between the polarized flux and system parameters, finding a few clear trends: presence of a companion drastically reduces the polarized flux levels, far-IR excess correlates with polarized flux for non-binary systems, and systems hosting disks with ring structures have stellar masses < 3 Msun. Our sample also included four hot, dusty "FS CMa" systems and we detected large-scale (> 100 au) scattered light around each, signs of extreme youth for these enigmatic systems. Science-ready images are publicly available through multiple distribution channels using a new FITS file standard jointly developed with members of the VLT/SPHERE team.

55. Optical and Near-Infrared Excesses are Correlated in T Tauri Stars

Kendall Sullivan, Adam L. Kraus ★ Accretion is one of the defining characteristics of classical T Tauri stars, fueled by the presence of a circumstellar disk comprised of dust and gas. Accretion produces a UV and optical excess, while re-radiated emission at the inner edge of the dust component of the disk produces a near-infrared (NIR) excess. The interplay between stars and their disks helps regulate protoplanetary disk evolution and dispersal, which is key to a full understanding of planet formation. To investigate the relations between NIR excess and optical excess in both single and binary stars, we used an archival sample of spectroscopically characterized members of the Taurus star-forming region ($\tau \sim$ 1-2 Myr) with measured luminosities, spectral types, and optical veiling. We combined the archival sample with 2MASS and WISE NIR photometry and high-resolution imaging surveys. We found that NIR and optical excesses are correlated in multiple NIR photometric bands, suggesting that they are closely related, likely because more massive disks have higher inner dust disk walls and are also associated with higher accretion rates. We also found that multiplicity has no impact on accretion or inner disk properties in a sample with a wide range of separations, but the sample was too small to specifically investigate close binaries, where the effects of multiplicity on disk properties should be most significant.

56. The Galactic dynamics revealed by the filamentary structure in atomic hydrogen emission

Juan D. Soler, Marc-Antoine Miville-Deschênes, Sergio Molinari, Ralf S. Klessen, Patrick Hennebelle, Leonardo Testi, Naomi M. McClure-Griffiths, Henrik Beuther, Davide Elia, Eugenio Schisano, Alessio Traficante, Philipp Girichidis, Simon C. O. Glover, Rowan J. Smith, Mattia Sormani, Robin Treß ★ We present a study of the filamentary structure in the atomic hydrogen (HI) emission at the 21 cm wavelength toward the Galactic plane using the observations in the HI4PI survey. Using the Hessian matrix method across radial velocity channels, we identified the filamentary structures and quantified their orientations using circular statistics. We found that the regions of the Milky Way's disk beyond 10 kpc and up to roughly 18 kpc from the Galactic center display HI filamentary structures predominantly parallel to the Galactic plane. For regions at lower Galactocentric radii, we found that the HI filaments are mostly perpendicular or do not have a preferred orientation with respect to the Galactic plane. We interpret these results as the imprint of supernova feedback in the inner Galaxy and Galactic rotation in the outer Milky Way. We found that the HI filamentary structures follow the Galactic warp and that they highlight some of the variations interpreted as the effect of the gravitational interaction with satellite galaxies. In addition, the mean scale height of the filamentary structures is lower than that sampled by the bulk of the HI emission, thus indicating that the cold and warm atomic hydrogen phases have different scale heights in the outer galaxy. Finally, we found that the fraction of the column density in HI filaments is almost constant up to approximately 18 kpc from the Galactic center. This is possibly a result of the roughly constant ratio between the cold and warm atomic hydrogen phases inferred from the HI absorption studies. Our results indicate that the HI filamentary structures provide insight into the dynamical processes shaping

the Galactic disk. Their orientations record how and where the stellar energy input, the Galactic fountain process, the cosmic ray diffusion, and the gas accretion have molded the diffuse interstellar medium in the Galactic plane.

57. Wavelike nature of the vertical shear instability in global protoplanetary disks

Eleonora Svanberg, Can Cui, Henrik N. Latter ★ The vertical shear instability (VSI) is a robust phenomenon in irradiated protoplanetary disks (PPDs). The majority of previous numerical simulations have focused on the turbulent properties of its saturated state. However, the saturation of the VSI manifests as large-scale coherent radially travelling inertial waves. In this paper, we study inertial-wave-disk interactions and their impact on VSI saturation. Inertial-wave linear theory is developed and applied to a representative global 2D simulation using the Athena++ code. It is found that the VSI saturates by separating the disk into several radial wave zones roughly demarcated by corotation resonances (turning points); this structure also manifests in modest radial variations in the vertical turbulence strength. Future numerical work should employ large radial domains to accommodate this radial structure of the VSI, while concurrently adopting sufficiently fine resolutions to resolve the parametric instability that attacks the saturated VSI inertial waves.

58. Pulsational instability of pre-main-sequence models from accreting protostars II. Modelling echelle diagrams of δ Scuti stars without rotational splitting

T. Steindl, K. Zwintz, M. Müllner ★ The physics of early stellar evolution (e.g. accretion processes) is often not properly included in the calculations of pre-main-sequence models, leading to insufficient model grids and hence systematic errors in the results. We aim to investigate current and improved approaches for the asteroseismic modelling of pre-main-sequence delta Scuti stars. We calculated an extensive grid of pre-main-sequence models including the early accretion phase and used the resulting equilibrium models as input to calculate theoretical frequency spectra. These spectra were used to investigate different approaches in modelling echelle diagrams to find the most reliable methods. By applying Petersen diagrams, we present a simple algorithm to extract echelle diagrams from observed pulsation frequencies. We show that model grids with insufficient input physics and imperfect modelling approaches lead to underestimated uncertainties and systematic errors in the extracted stellar parameters. Our re-discussion of HD 139614 leads to different stellar parameters than the ones derived by Murphy et al. (2021). We performed a model comparison between this previous investigation and our results by applying the Akaike and Bayesian information criteria. While the results with regard to our 10-d model are inconclusive, they show (very) strong evidence of a 6-d model with fixed accretion parameters (leading to almost identical stellar parameters to those of the 10-d model) to be preferred over the model applied by Murphy et al. (2021). In general, our modelling approach can provide narrow constraints on the stellar parameters (Δ R $\sim$ 0.05 R$_\odot$, Δ log g $<$ 0.01, and Δ M$_\star$ 0.1 M$_\odot$). The extensively tested modelling approaches and automatic extraction of echelle diagrams should allow us to study many more pre-main-sequence delta Scuti stars in the future and lead to reliable stellar parameters.

59. How cooling influences circumbinary discs

Prakruti Sudarshan, Anna B. T. Penzlin, Alexandros Ziampras, Wilhelm Kley, Richard P. Nelson ★ Circumbinary disc observations and simulations show large, eccentric inner cavities. Recent work has shown that the shape and size of these cavities depend on the aspect ratio and viscosity of the disc, as well as the binary eccentricity and mass ratio. It has been further shown that, for gaps created by planets, the cooling timescale significantly affects the shape and size of the gap. In this study, we consider the effect of different cooling models on the cavity shape in a circumbinary disc. We compare locally isothermal and radiatively cooled disc models to ones with a parametrised cooling timescale (β-cooling), implemented in 2D numerical simulations for varying binary eccentricities. While the shape of the cavity for radiative and locally isothermal models remains comparable, the inner disc structure changes slightly, leading to a change in the precession rate of the disc. With β-cooled models, the shape and size of the cavity changes dramatically towards values of β=1. Based on our findings, we introduce a parametrised β model that accounts for the shorter cooling timescale inside the cavity while adequately reproducing the results of the radiative model, and we highlight that accurate treatment of the thermodynamics inside the cavity has a significant impact in modelling circumbinary systems.

60. Nonradial and nonpolytropic astrophysical outflows. XI. Simulations of the circumstellar environment of RY Tau

C. Sauty, R. M. G. de Albuquerque, V. Cayatte, J. J. G. Lima, J. F. Gameiro ★ Context. There are recent observational evidences that RY Tau may present two different outflow stages, a quiescent one and a more active one. We try to model that phenomenon. Aims. We have performed new 2.5D magneto-hydrodynamical simulations of the possible accretion-outflow environment of RY Tau based on analytical solutions to reduce the relaxation time. Methods. We used as initial conditions the analytical self-similar solution we used to model the RY Tau micro jet. In the closed field line region of the magnetosphere we have reversed the direction of the flow and increased the accretion rate by increasing the density and the velocity. We have also implemented the heating rate and adjusted it according to the velocity of the flow. The accretion disk is treated as a boundary

condition. Results. The simulations show that the stellar jet and the accreting magnetosphere attain a steady state in only a few stellar rotations, confirming the robustness and stability of self-similar solutions. Additionally, two types of behavior were observed similar to the one observed in RY Tau. Either the steady stellar outflow and magnetospheric inflow are separated by a low static force free region or the interaction between the stellar jet and the magnetospheric accretion creates coronal episodic mass ejections originating from the disk and bouncing back onto the star. Conclusions. The ratio of mass loss rate to mass accretion rate that coincides with the change of behaviour observed in RY Tau, lays within the range of ratios that have been measured during the period of the micro jet initial analysis.

61. A graph theory-based multi-scale analysis of hierarchical cascade in molecular clouds : Application to the NGC 2264 region

B. Thomasson, I. Joncour, E. Moraux, C. Crespelle, F. Motte, Y. Pouteau, T. Nony ★ The spatial properties of small star-clusters suggest that they may originate from a fragmentation cascade of the cloud for which there might be traces up to a few dozen of kAU. Our goal is to investigate the multi-scale spatial structure of gas clumps, to probe the existence of a hierarchical cascade and to evaluate its possible link with star production in terms of multiplicity. From the Herschel emission maps of NGC 2264, clumps are extracted using getsf software at each of their associated spatial resolution, respectively [8.4, 13.5, 18.2, 24.9, 36.3]". Using the spatial distribution of these clumps and the class 0/I Young Stellar Object (YSO) from Spitzer data, we develop a graph-theoretic analysis to represent the multi-scale structure of the cloud as a connected network. From this network, we derive three classes of multi-scale structure in NGC 2264 depending on the number of nodes produced at the deepest level: hierarchical, linear and isolated. The structure class is strongly correlated with the column density $N_{\rm H_2}$ since the hierarchical ones dominate the regions whose $\rm N_{H_2} > 6 \times 10^{22} cm^{-2}$. Although the latter are in minority, they contain half of the class 0/I YSOs proving that they are highly efficient in producing stars. We define a novel statistical metric, the fractality coefficient F that measure the fractal index describing the scale-free process of the cascade. For NGC 2264, we estimate F = 1.45±0.12. However, a single fractal index fails to fully describe a scale-free process since the hierarchical cascade starts at a 13 kAU characteristic spatial scale. Our novel methodology allows us to correlate YSOs with their multi-scale gaseous environment. This hierarchical cascade that drives efficient star formation is suspected to be both hierarchical and rooted by the larger-scale gas environment up to 13 kAU.

62. The Musca molecular cloud: The perfect "filament" is still a sheet

A. Tritsis, F. Bouzelou, R. Skalidis, K. Tassis, T. Enßlin, G. Edenhofer ★ The true 3-dimensional (3D) morphology of the Musca molecular cloud is a topic that has received significant attention lately. Given that Musca does not exhibit intense star-formation activity, unveiling its shape has the potential of also revealing crucial information regarding the physics that dictates the formation of the first generation of stars within molecular clouds. Here, we revisit the shape of Musca and we present a comprehensive array of evidence pointing towards a shape that is extended along the line-of-sight dimension: (a) 3D maps of differential extinction; (b) new non-local thermodynamic equilibrium radiative transfer simulations of CO rotational transitions from a sheet-like, magnetically-dominated simulated cloud; (c) an effective/critical density analysis of available CO observations; (d) indirect consequences that a filamentary structure would have had, from a theoretical star-formation perspective. We conclude that the full collection of observational evidence strongly suggests that Musca has a sheet-like geometry.

63. Hot methanol in the [BHB2007] 11 protobinary system: hot corino versus shock origin? : FAUST V

C. Vastel et al. - FAUST team ★ Methanol is a ubiquitous species commonly found in the molecular interstellar medium. It is also a crucial seed species for the building-up of the chemical complexity in star forming regions. Thus, understanding how its abundance evolves during the star formation process and whether it enriches the emerging planetary system is of paramount importance. We used new data from the ALMA Large Program FAUST (Fifty AU STudy of the chemistry in the disk/envelope system of Solar-like protostars) to study the methanol line emission towards the [BHB2007] 11 protobinary system (sources A and B), where a complex structure of filaments connecting the two sources with a larger circumbinary disk has been previously detected. Twelve methanol lines have been detected with upper energies in the range [45-537] K along with one 13CH3OH transition. The methanol emission is compact and encompasses both protostars, separated by only 28 au and presents three velocity components, not spatially resolved by our observations, associated with three different spatial regions, with two of them close to 11B and the third one associated with 11A. A non-LTE radiative transfer analysis of the methanol lines concludes that the gas is hot and dense and highly enriched in methanol with an abundance as high as 1e-5. Using previous continuum data, we show that dust opacity can potentially completely absorb the methanol line emission from the two binary objects. Although we cannot firmly exclude other possibilities, we suggest that the detected hot methanol is resulting from the shocked gas from the incoming filaments streaming towards [BHB2007] 11 A and B, respectively. Higher spatial resolution observations are necessary to confirm this hypothesis.

64. The growth and migration of massive planets under the influence of external photoevaporation

Andrew J. Winter, Thomas J. Haworth, Gavin A. L. Coleman, Sergei Nayakshin ★ The formation of gas giant planets must occur during the first few Myr of a star's lifetime, when the protoplanetary disc still contains sufficient gas to be accreted onto the planetary core. The majority of protoplanetary discs are exposed to strong ultraviolet irradiation from nearby massive stars, which drives winds and depletes the mass budget for planet formation. It remains unclear to what degree external photoevaporation affects the formation of massive planets. In this work, we present a simple one dimensional model for the growth and migration of a massive planet under the influence of external FUV fields. We find that even moderate FUV fluxes $F_{\rm FUV} \gtrsim 100\,G_0$ have a strong influence on planet mass and migration. By decreasing the local surface density and shutting off accretion onto the planet, external irradiation suppresses planet masses and halts migration early. The distribution of typical stellar birth environments can therefore produce an anti-correlation between semi-major axis and planet mass, which may explain the apparent decrease in planet occurrence rates at orbital periods $P_{\rm orb} \gtrsim 10^3$ days. Even moderate fluxes $F_{\rm FUV}$ strongly suppress giant planet formation and inward migration for any initial semi-major axis if the stellar host mass $M_* \lesssim 0.5\,M_\odot$, consistent with findings that massive planet occurrence is much lower around such stars. The outcomes of our prescription for external disc depletion show significant differences to the current approximation adopted in state-of-the-art population synthesis models, motivating future careful treatment of this important process.

65. The 30 Doradus Molecular Cloud at 0.4 pc Resolution with the Atacama Large Millimeter/submillimeter Array: Physical Properties and the Boundedness of CO-emitting Structures

Tony Wong, Luuk Oudshoorn, Eliyahu Sofovich, Alex Green, Charmi Shah, Rémy Indebetouw, Margaret Meixner, Alvaro Hacar, Omnarayani Nayak, Kazuki Tokuda, Alberto D. Bolatto, Mélanie Chevance, Guido De Marchi, Yasuo Fukui, Alec S. Hirschauer, K. E. Jameson, Venu Kalari, Vianney Lebouteiller, Leslie W. Looney, Suzanne C. Madden, Toshikazu Onishi, Julia Roman-Duval, Mónica Rubio, A. G. G. M. Tielens ★ We present results of a wide-field (approximately 60 x 90 pc) ALMA mosaic of CO(2-1) and ^{13}CO(2-1) emission from the molecular cloud associated with the 30 Doradus star-forming region. Three main emission complexes, including two forming a bowtie-shaped structure extending northeast and southwest from the central R136 cluster, are resolved into complex filamentary networks. Consistent with previous studies, we find that the central region of the cloud has higher line widths at fixed size relative to the rest of the molecular cloud and to other LMC clouds, indicating an enhanced level of turbulent motions. However, there is no clear trend in gravitational boundedness (as measured by the virial parameter) with distance from R136. Structures observed in ^{13}CO are spatially coincident with filaments and are close to a state of virial equilibrium. In contrast, CO structures vary greatly in virialization, with low CO surface brightness structures outside of the main filamentary network being predominantly unbound. The low surface brightness structures constitute 10remnants of previously star-forming gas clumps, or alternatively the CO-emitting parts of more massive, CO-dark structures.

66. A new method for direct measurement of isotopologue ratios in protoplanetary disks: a case study of the ^{12}CO/^{13}CO ratio in the TW Hya disk

Tomohiro C. Yoshida, Hideko Nomura, Kenji Furuya, Takashi Tsukagoshi, Seokho Lee ★ Planetary systems are thought to be born in protoplanetary disks. Isotope ratios are a powerful tool for investigating the material origin and evolution from molecular clouds to planetary systems via protoplanetary disks. However, it is challenging to measure the isotope (isotopologue) ratios, especially in protoplanetary disks, because the emission lines of major species are saturated. We developed a new method to overcome these challenges by using optically thin line wings induced by thermal broadening. As a first application of the method, we analyzed two carbon monoxide isotopologue lines, ^{12}CO $3-2$ and ^{13}CO $3-2$, from archival observations of a protoplanetary disk around TW Hya with the Atacama Large Millimeter/sub-millimeter Array. The ^{12}CO/^{13}CO ratio was estimated to be 20 ± 5 at disk radii of $70-110$ au, which is significantly smaller than the value observed in the local interstellar medium, ~ 69. It implies that an isotope exchange reaction occurs in a low-temperature environment with C/O > 1 . In contrast, it is suggested that ^{12}CO/^{13}CO is higher than ~ 84 in the outer disk ($r > 130$ au), which can be explained by the difference in the binding energy of the isotopologues on dust grains and the CO gas depletion processes. Our results imply that the gas-phase ^{12}CO/^{13}CO can vary by a factor of > 4 even inside a protoplanetary disk, and therefore, can be used to trace material evolution in disks.

67. Molecular Gas Structures traced by ^{13}CO Emission in the 18,190 ^{12}CO Molecular Clouds from the MWISP Survey

Lixia Yuan, Ji Yang, Fujun Du, Yang Su, Xunchuan Liu, Shaobo Zhang, Yan Sun, Xin Zhou, Qing-Zeng Yan, Yuehui Ma ★ After the morphological classification of the 18,190 ^{12}CO molecular clouds, we further investigate the properties of their internal molecular gas structures traced by the ^{13}CO($J = 1-0$) line emissions. Using three different methods to extract

the ^{13}CO gas structures within each ^{12}CO cloud, we find that $\sim$ 15% of ^{12}CO clouds (2851) have ^{13}CO gas structures and these ^{12}CO clouds contribute about 93% of the total integrated flux of ^{12}CO emission. In each of 2851 ^{12}CO clouds with ^{13}CO gas structures, the ^{13}CO emission area generally does not exceed 70% of the ^{12}CO emission area, and the ^{13}CO integrated flux does not exceed 20% of the ^{12}CO integrated flux. We reveal a strong correlation between the velocity-integrated intensities of ^{12}CO lines and those of ^{13}CO lines in both ^{12}CO and ^{13}CO emission regions. This indicates the H_2 column densities of molecular clouds are crucial for the ^{13}CO lines emission. After linking the ^{13}CO structure detection rates of the 18,190 ^{12}CO molecular clouds to their morphologies, i.e. nonfilaments and filaments, we find that the ^{13}CO gas structures are primarily detected in the ^{12}CO clouds with filamentary morphologies. Moreover, these filaments tend to harbor more than one ^{13}CO structure. That demonstrates filaments not only have larger spatial scales, but also have more molecular gas structures traced by ^{13}CO lines, i.e. the local gas density enhancements. Our results favor the turbulent compression scenario for filament formation, in which dynamical compression of turbulent flows induces the local density enhancements. The nonfilaments tend to be in the low-pressure and quiescent turbulent environments of the diffuse interstellar medium.

68. Dependence of Molecular Cloud Samples on Angular Resolution, Sensitivity, and Algorithms

Qing-Zeng Yan, Ji Yang, Yang Su, Yan Sun, Xin Zhou, Ye Xu, Hongchi Wang, Shaobo Zhang, Zhiwei Chen
★ In this work, we investigate the observational and algorithmic effects on molecular cloud samples identified from position-position-velocity (PPV) space. By smoothing and cutting off the high quality data of the Milky Way Imaging Scroll Painting (MWISP) survey, we extract various molecular cloud samples from those altered data with the DBSCAN (density-based spatial clustering of applications with noise) algorithm. Those molecular cloud samples are subsequently used to gauge the significance of sensitivity, angular/velocity resolution, and DBSCAN parameters. Two additional surveys, the FCRAO Outer Galaxy Survey (OGS) and the CfA-Chile 1.2 m complete CO (CfA-Chile) survey, are used to verify the MWISP results. We found that molecular cloud catalogs are not unique and the boundary and therefore the number shows strong variation with angular resolution and sensitivity. At low angular resolution (large beam sizes), molecular clouds merge together in PPV space, while low sensitivity (high cutoffs) misses small faint molecular clouds and takes bright parts of large molecular clouds as single ones. At high angular resolution and sensitivity, giant molecular clouds (GMCs) are resolved into individual clouds, and their diffuse components are also revealed. Consequently, GMCs are more appropriately interpreted as clusters or aggregates of molecular clouds, i.e., GMCs represent molecular cloud samples themselves.

69. Two Candidate KH 15D-like Systems from the Zwicky Transient Facility

Wei Zhu, Klaus Bernhard, Fei Dai, Min Fang, J. J. Zanazzi, Weicheng Zang, Subo Dong, Franz-Josef Hambsch, Tianjun Gan, Zexuan Wu, Michael Poon
★ KH 15D contains a circumbinary disk that is tilted relative to the orbital plane of the central binary. The precession of the disk and the orbital motion of the binary together produce rich phenomena in the photometric light curve. In this work, we present the discovery and preliminary analysis of two objects that resemble the key features of KH 15D from the Zwicky Transient Facility. These new objects, Bernhard-1 and Bernhard-2, show large-amplitude (> 1.5 mag), long-duration (more than tens of days), and periodic dimming events. A one-sided screen model is developed to model the photometric behaviour of these objects, the physical interpretation of which is a tilted, warped circumbinary disk occulting the inner binary. Changes in the object light curves suggest potential precession periods over timescales longer than 10 years. Additional photometric and spectroscopic observations are encouraged to better understand the nature of these interesting systems.

70. Magnetic Field of Molecular Gas Measured with the Velocity Gradient Technique I. Orion A

Mengke Zhao, Jianjun Zhou, Yue Hu, A. Lazarian, Xindi Tang, Willem A. Baan, Jarken Esimbek, Yuxin He, Dalei Li, Weiguang Ji, Kadirya Tursun
★ Magnetic fields play an important role in the evolution of molecular clouds and star formation. Using the Velocity Gradient Technique (VGT) model, we measured the magnetic field in Orion A using the 12CO, 13CO, and C18O (1-0) emission lines at a scale of 0.07 pc. The measured B-field shows an east-west orientation that is perpendicular to the integral shaped filament of Orion A at large scale. The VGT magnetic fields obtained from 13CO and C18O are in agreement with the B-field that is measured from the Planck 353 GHz dust polarization at a scale of 0.55 pc. Removal of density effects by using a Velocity Decomposition Algorithm can significantly improve the accuracy of the VGT in tracing magnetic fields with the 12CO (1-0) line. The magnetic field strength of seven sub-clouds, OMC-1, OMC-2, OMC-3, OMC-4, OMC-5, L 1641-N, and NGC 1999 has also been estimated with the Davis-Chandrasekhar-Fermi (DCF) and MM2 technique, and these are found to be in agreement with previous results obtained from dust polarization at far-infrared and sub-millimeter wavelengths. At smaller scales, the VGT proves a good method to measure magnetic fields.

71. ATOMS: ALMA Three-millimeter Observations of Massive Star-forming regions – XI. From inflow to infall in hub-filament systems

Jian-Wen Zhou et al. ★ We investigate the presence of hub-filament systems in a large sample of 146 active proto-clusters, using $H^{13}CO^+$ J=1-0 molecular line data obtained from the ATOMS survey. We find that filaments are ubiquitous in proto-clusters, and hub-filament systems are very common from dense core scales (∼0.1 pc) to clump/cloud scales (∼1-10 pc). The proportion of proto-clusters containing hub-filament systems decreases with increasing dust temperature (T_d) and luminosity-to-mass ratios (L/M) of clumps, indicating that stellar feedback from HII regions gradually destroys the hub-filament systems as proto-clusters evolve. Clear velocity gradients are seen along the longest filaments with a mean velocity gradient of 8.71 km $s^{-1}pc^{-1}$ and a median velocity gradient of 5.54 km $s^{-1}pc^{-1}$. We find that velocity gradients are small for filament lengths larger than ∼1 pc, probably hinting at the existence of inertial inflows, although we cannot determine whether the latter are driven by large-scale turbulence or large-scale gravitational contraction. In contrast, velocity gradients below ∼1 pc dramatically increase as filament lengths decrease, indicating that the gravity of the hubs or cores starts to dominate gas infall at small scales. We suggest that self-similar hub-filament systems and filamentary accretion at all scales may play a key role in high-mass star formation.

72. The Pre-main Sequence: Challenges and Prospects for Asteroseismology

Konstanze Zwintz, Thomas Steindl ★ Stars do not simply pop up on the main sequence. Before the stars arrive on the zero-age main sequence, they form in the collapses of molecular clouds, gain matter through accretion processes, and compress their cores until hydrogen can burn in full equilibrium. Although this evolutionary phase lasts a relatively short time, it is the imprint of these important physical processes that is often ignored by simplified assumptions. While asteroseismology offers a great tool to investigate these physical processes, studying pre-MS oscillations in turn has the potential to further advance the field. Asteroseismology of pre-main sequence stars faces observational and theoretical challenges. The remnants of their birth environment which is often still surrounding the young stars causes variability that can interfere with the signal of pulsations. The lack of long time-base satellite observations in addition limits the applications of the method. Theoretical models of pre-main sequence stars include several assumptions and simplifications that influence the calculation of pulsation frequencies and excitation properties of pulsation modes. Keeping all this in mind, the prospects for pre-main sequence asteroseismology are manifold. An improved understanding of the structure of young stellar objects has the potential to answer some of the open questions of stellar evolution, including angular momentum transport and the formation of magnetic fields. While gyrochronology, for example, struggles to determine the ages of the youngest clusters, pulsations in pre-main sequence stars can function as an independent age indicator yielding higher precision for single stars. The increasing interest of stellar astrophysics in general to investigate the formation and early evolution of stars and planets illustrates the growing importance of pre-main sequence asteroseismology.